Drug Design, Development and Therapy

Dovepress
open access to scientific and medical research

Open Access Full Text Article

ORIGINAL RESEARCH

RETRACTED ARTICLE: Preparation, in vitro and in vivo Evaluation of Thermosensitive in situ Gel Loaded with Ibuprofen-Solid Lipid Nanoparticles for Rectal Delivery

Chun-hui Huang[1,2,*], Peng-yi Hu[2,3,*], Qiu-yan Wu[2,3], Ming-yan Xia[2,3], Wen-li Zhang[3], Zhi-qiang Lei[3], Dong-xun Li[3], Guo-song Zhang[2,3], Jian-fang Feng[1,2]

[1]School of Pharmacy, Guangxi University of Chinese Medicine, Nanning, Guangxi, 530200, People's Republic of China; [2]National Engineering Research Center of Chinese Medicine Solid Preparation Manufacturing Technology, Nanchang, 330006, People's Republic of China; [3]Jiangxi University of Traditional Chinese Medicine, Nanchang, 330004, People's Republic of China

*These authors contributed equally to this work

Correspondence: Guo-song Zhang, National Engineering Research Center of Chinese Medicine Solid Preparation Manufacturing Technology, Nanchang, 330006, People's Republic of China, Email zhgs81411@aliyun.com; Jian-fang Feng, School of Pharmacy, Guangxi University of Chinese Medicine, Nanning, 530200, People's Republic of China, Email fengjianfang@vip.163.com

Background: Ibuprofen (IBU), a nonsteroidal anti-inflammatory drug, shows poor gastrointestinal absorption due to its low solubility, which limits its clinical application.

Objective: In the present study, we aimed to develop thermosensitive gel-mediated ibuprofen-solid lipid nanoparticles (IBU-SLN-ISG) to improve the dissolution and bioavailability of IBU after rectal delivery.

Methods: IBU-loaded SLNs (IBU-SLNs) were developed and optimized applying Box-Behnken design. The optimized IBU-SLNs were characterized by physicochemical parameters and morphology. Then, the optimized IBU-SLNs was incorporated into the gel and characterized for gel properties and rheology and investigated its release in vitro, pharmacokinetics in vivo, rectal irritation and rectal retention time.

Results: The optimized SLNs had an EE of 90.74 ± 1.20%, DL of 11.36 ± 1.20%, MPS of 166.77 ± 2.26 nm, PDI of 0.27 ± 0.08, and ZP of −21.00 ± 0.59 mV. The FTIR spectra confirmed successful encapsulation of the drug inside the nanoparticle as only peaks responsible for the lipid could be identified. This corroborated well with XRD spectra, which showed a completely amorphous state of the IBU-SLNs as compared to the crystalline nature of the pure drug. The gelation temperature of the prepared IBU-SLN-ISG was 33.30 ± 0.78°C, the gelation time was 14.67 ± 2.52 s, the gel strength was 54.00 ± 1.41 s, and the mucoadhesion was (11.54±0.37) × 10^2dyne/cm^2. The in vitro results of IBU-SLNs and IBU-SLN-ISG showed a biphasic release pattern with initial burst release followed by sustained release. More importantly, IBU-SLN-ISG produced much better absorption of IBU and improved bioavailability in rats. In addition, IBU-SLN-ISG caused no irritation damage to rectal tissues, and could be retained in the rectum for a long time.

Conclusion: Thermosensitive in situ gel loaded with IBU-solid lipid nanoparticles might be further developed as a more convenient and effective rectal dosage form.

Keywords: thermosensitive gel, ibuprofen, solid lipid nanoparticle, rectal delivery, bioavailability

Introduction

Ibuprofen (IBU), a nonsteroidal anti-inflammatory drug (NSAID), is a nonselective cyclooxygenase (COX) inhibitor, exerts potent pyrolysis, analgesic and anti-inflammatory effects after oral or rectal administration.[1] It could be used to treat rheumatoid arthritis, various forms of joint and non-articular rheumatism, as well as pain caused by inflammatory peripheral nervous system involvement, exacerbation of gout, neuralgia, myalgia, ankylosing spondylitis, radiculitis, and

Received: 24 December 2021
Accepted: 27 April 2022
Published: 12 May 2022

trauma.[2] It is most prescribed for the treatment of fever and moderate pain in childhood. However, IBU is evaluated as a BCSII drug according to the Biopharmaceutical Classification System (BCS). IBU shows poor gastrointestinal absorption due to the low solubility or dissolution rate to water (21 mg/L at 25°C).[3] And it is rapidly bio-transformed with a serum half-life of 1.8 to 2 hours, which means that patients are required to administer it three to five times daily.[4] Therefore, finding a desirable delivery is necessary to ameliorate these defects.

Rectal route offers a noninvasive and useful route for drug administration when systemic or local effects are required. The rectum offers a relatively constant environment for drug delivery that allows a constant steady-state concentration of drug in plasma and partially avoids hepatic first-pass effect or gastrointestinal drug absorption difficulties.[5,6] Suppositories, a common form of rectal administration, have been favorable dosage forms for infants, children and unconscious patients. However, the use of conventional solid suppositories is often accompanied by discomfort. Furthermore, conventional solid suppositories might reach the end of the colon and make the carried drugs experience the first-pass effect.[7] In addition, rectal administration of liquid forms often causes anal leakage, leading to inadequate dosing.[8] To overcome these deficiencies, there have been several attempts to develop suppositories which exist as liquid at room temperature but gel in the body, by modulating the gelation temperatures of poloxamer solutions.[7] The development of a new thermosensitive liquid suppository has prompted investigation of many drugs with this new method of delivery: indomethacin,[8] acetaminophen,[10,11] diclofenac sodium,[5,6,12] propranolol,[14] quinine,[15] insulin,[16–18] carbamazepine,[19] diltiazem hydrochloride,[20] etodolac[21] nimesulide,[22] flurbiprofen[8,23] and tramadol hydrochloride.[24] However, since IBU is a poorly water-soluble drug, we have to increase its rectal absorption by applying some formulation strategies to improve that.

There are many approaches to enhance the solubility of IBU, such as mechanical micritization,[20] solid dispersion,[21] and self-emulsifying drug delivery system. Recently, solid lipid nanoparticles (SLNs) gel system may serve as a solution to overcome the limitations of the solubility related low bioavailability of IBU. SLNs can comprise physiological and biodegradable lipids, which were earlier reported to possess low systemic toxicity and low cytotoxicity.[11,26] The small size of the lipid nanoparticles ensures close contact between the lipid particles and the lipid bilayer of the rectum, resulting in the penetration of an increased amount of drug into the body. As a base of liquid suppositories, Poloxamer solutions are known to exhibit the phenomenon of reverse thermal gelation, remaining as solutions at low temperature and gelling when temperature increases.[13] Furthermore, poloxamers were reported not to cause any damage to mucosal membranes.[26,28] To modulate the gel strength of IBU-SLNs-ISG, bioadhesive polymers such as, hydroxypropyl methylcellulose (HPMC) and hyaluronic acid (HA) were studied.

The aim of this study was to develop thermosensitive gel loaded with ibuprofen-solid lipid nanoparticles (IBU-SLN-ISG) for prolonging IBU residence time and improving its bioavailability after rectal delivery. The physicochemical properties of IBU-SLN were characterized by means of techniques, such as X-ray diffraction (XRD), size distribution, zeta potential, gelation temperature, gel strength and in vitro dissolution. Furthermore, the in vivo pharmacokinetics and rectal tissue irritation of IBU in situ gel (IBU-ISG) and IBU-SLN-ISG were also investigated and compared.

Materials and Methods

Materials

Ibuprofen (IBU, content 99.9%) was purchased from Shandong Xinhua Pharmaceutical Co., Ltd. (Zibo, China). Stearic acid and glycerol monostearate were obtained from Shanghai Qingxi Chemical Technology Co., Ltd. (Shanghai, China). Hyaluronic acid was obtained from Shanxi Tengmai Biological Technology Co., Ltd. (Xi'an, China). Poloxamer 407 and Poloxamer 188 were acquired from BASF (Ludwigshafen, Germany). Purified water was used after deionization and filtration in a Millipore VR system. Tween 80 was purchased from Sichuan Jinshan Pharmaceutical Co., Ltd. (Sichuan, China). Acetonitrile and methanol of HPLC grade were purchased from Fisher Scientific. Paediatric Ibuprofen Suppository was obtained from Shanxi Taiyuan Pharmaceutical Co., Ltd. All other chemical reagents and solvents used were of analytical grade.

Preparation of Ibuprofen-Solid Lipid Nanoparticles

The solid lipid nanoparticles loaded with IBU were prepared by a hot homogenization method.[29] Briefly, IBU was dissolved in a mixture of stearic acid (SA) and glyceryl monostearate (GMS) in a water bath at 70°C to form the lipid phase. The surfactant Tween 80 was dissolved in purified water at the same temperature to form the aqueous phase. Then, the aqueous phase was added to the lipid phase, and the mixture was stirred with an IKA EUROSTAR digital stirrer at 1000 rpm for 15 minutes in a 70°C-water bath to obtain a primary emulsion. Afterward, the obtained pre-emulsion was sonicated using a probe sonicator (Ultrasonic Homogenizer JY92-IIN) at 50% of amplitude during 10 minutes to obtain a nanoemulsion. Next, the hot nanoemulsion was magnetically stirred for 10 min in an ice bath to recrystallize the lipid and form the SLNs solution. The obtained IBU-SLNs solution was freeze-dried in a freeze dryer (EYELA-FDU-2100, Japan) and was analyzed by SEM, XRD and FTIR method. The process was that the IBU-SLNs solution was frozen at −50°C for 48 h in the lyophilizer chamber followed by primary drying at −35°C and 150 mtorr for 24 h, followed by a secondary drying at 15°C and 50 mtorr for 6 h. The detailed composition of IBU-SLNs is given in Table 1.

Optimization of Ibuprofen-Solid Lipid Nanoparticles

The optimization of IBU-SLNs formulation parameters were studied by Box-Behnken design using software Design-Expert 8.0.6.[30] Based on the results obtained in preliminary experiments, three independent variables were found to be the major variables in determining the encapsulation efficiency and drug loading. The three independent variables were the amount of stearic acid (A), glyceryl monostearate (B) and surfactant Tween 80 (C). According to the design, 17 IBU-SLN preparations were formed, and optimized by the results of encapsulation efficiency (EE, R1), drug loading (DL, R2), mean particle size (MPS, R3), polymer dispersity index (PDI, R4) and zeta potential (ZP, R5) (Table 2). The optimized formulation was predicted by the fitness of the model among the linear (main effects only), two-factor interaction (effects and interactions) and quadratic models (effects, interactions and quadratic terms). Based on the best-fitting model, a polynomial equation suitable for each response was determined and used to evaluate the influence of the independent variable on the studied response. A model with a p-value of less than 0.05 was considered statistically significant. The objective function of this research was to maximize the EE and DL, and minimize MPS, PDI and ZP.

Physicochemical Properties of IBU-SLNs

Particle Size, Polydispersity Index and Zeta Potential

The mean particle size and polydispersity index of IBU-SLNs were investigated at 25°C and at a scattering angle of 90°. After equilibration for 30 seconds by dynamic light scattering using Zetasizer (Nano ZS 3690, Malvern Instruments, UK) furnished with a He–Ne laser that operated at a wavelength of 633 nm.[57] Prior to measurements of each sample, the IBU-SLNs dispersion (10 μL) was disseminated in 2 mL of ultra-purified water, then sonicated for a few minutes to produce

Table Variables and Their Levels in the Box-Behnken Design

	Levels		
	−1	0	1
Independent variables			
A=Amount of stearic acid (g)	0.1	0.2	0.3
B=Amount ofglyceryl monostearate (g)	0.1	0.2	0.3
C=Amount of Tween 80 (g)	0.2	0.4	0.6
Dependent variables	Constraints		
R1=Encapsulation efficiency (EE%)	Maximize		
R2= Drug loading (DL%)	Maximize		
R3=mean particle size (MPS, nm)	Minimize		
R4=polymer dispersity index (PDI)	Minimize		
R5=zeta potential (ZP, mV)	Minimize		

Table 2 Box-Behnken Experimental Design and the Effects of Different Formulation Variables on EE (R1), DL (R2), MPS (R3), PDI (R4), ZP (R5)

Run	Actual Value Variables			Response Values				
	A (g)	B (g)	C (g)	R1 (%)	R2 (%)	R3 (nm)	R4	R5 (mV)
1	0.2	0.2	0.4	87.61	11.93	188.57	0.45	−21.3
2	0.2	0.1	0.6	85.48	7.04	110.50	0.73	−24.37
3	0.2	0.3	0.6	86.43	9.54	95.50	0.24	−18.8
4	0.1	0.2	0.2	80.46	10.09	184.80	0.41	−18.77
5	0.1	0.2	0.6	83.45	7.20	114.83	0.35	−17.8
6	0.3	0.3	0.4	87.26	11.35	119.40	0.35	−15.0
7	0.1	0.3	0.4	81.55	9.51	119.70	0.38	−17.53
8	0.2	0.2	0.4	89.53	14.90	273.67	[illegible]	−20.8
9	0.2	0.2	0.4	88.79	14.94	217.17	0.58	−19.3
10	0.2	0.2	0.4	87.18	13.30	196.57	[illegible]	−20.4
11	0.2	0.1	0.2	72.72	7.72	189.07	[illegible]	−18.57
12	0.3	0.1	0.4	81.12	7.25	15[illegible]	0.39	−18.53
13	0.3	0.2	0.2	76.09	7.18	[illegible]	0.77	−22.1
14	0.2	0.3	0.2	84.10	10.68	168.[illegible]	[illegible]	−15.5
15	0.3	0.2	0.6	90.28	8.25	201.47	[illegible]	−17.3
16	0.2	0.2	0.4	85.46	13.[illegible]	219.43	0.44	−20.3
17	0.1	0.1	0.4	83.59	12.65	[illegible]	0.35	−15.73

a suitable scattering intensity.[38] The zeta potential of IBU-SLNs was determined using the same instrument based on an electrophoretic light scattering technique.[27] In this study, the results were determined three times and reported as mean ± standard deviation (SD).

Encapsulation Efficiency and Drug Loading

The encapsulation efficiency and drug loading of IBU-SLNs were determined by ultrafiltration and centrifugation. Briefly, 100 μL of IBU-SLNs formulation was mixed in 400 μL of Milli-Q water in an ultrafiltration centrifuge tube (MWCO = 10 kDa; Solarbio Technology Co., Ltd., Beijing). And then the samples were centrifuged (Eppendorf Centrifuge 5410 R) at 12,000 rpm for 20 minutes at 4°C. Afterward, the filtrate then was diluted with methanol and was labeled as W_{free}. To measure the total amount of IBU in IBU-SLNs, 1 mL of formulation were diluted in 5 mL of methanol and sonicated for 30 min to dissolve the entrapped SLNs, and was labeled as W_{total}. All the samples were filtered through a 0.22-μm membrane and then analyzed by a Shimadzu LC-20AT high performance liquid chromatography system (HPLC) to investigate the content of IBU. The entrapment efficiency was calculated using the following equations:

Entrapment efficiency (EE) (%): $EE(\%) = \frac{W_{total} - W_{free}}{W_{total}} \times 100$

Drug loading (DL) (%): $DL(\%) = \frac{W_{total} - W_{free}}{W_{lipid}} \times 100$

where W_{total} represents the total amount of IBU in IBU-SLNs, W_{free} represents the free amount of IBU in IBU-SLNs, and W_{lipid} represents the total amount of lipid nanoparticle.

HPLC Analysis of IBU

The content of IBU was determined by the HPLC method. The HPLC instrumentation included a CBM-20Alite system controller, a Shimadzu LC-20AT solvent delivery system, a Shimadzu SPD-M20A UV/VIS photodiode array detector, a Shimadzu SIL-20A auto injector and a Shimadzu CTO-20A column oven. The chromatographic data were collected and processed by means of Shimadzu LC solution software (Shimadzu Corp). A Hypersil (4.6 × 250 mm, 5 μm) analytical column was used. The eluate was monitored at 263 nm. The mobile phase was an acetonitrile-sodium acetate

buffer (pH adjusted to 2.5 with acetic acid) (60:40, v/v) with a flow speed of 1.0 mL/min. The injection volume was 20 μL, and the column temperature was 35°C. The run time was 10 minutes and the retention time of IBU was approximately 5.4 minutes. A linear correlation was acquired between peak area and concentration. The linear equation was y=447.69x-4703.6 (R^2=0.9992), where x is the concentration and y is the peak area. The assay was linear in the concentration of 1.0~150 μg/mL. The limit of detection was 0.5 μg/mL.

Scanning Electron Microscope (SEM)

The shape and surface topography of IBU and IBU-SLNs were determined using scanning electron microscope (FP 2012/14 Quanta250; SE DETECTOR R580; USA) operating at 13kV. The freeze-dried IBU-SLNs powder was mounted on a metal stub with double-sided adhesive tape and gold-coated under vacuum in an argon atmosphere prior to observation.[34]

X-Ray Powder Diffraction (XRD)

X-ray powder diffraction technique was used to analyze the crystal structure of the prepared formulation. To study the change in the crystalline state, IBU, lipid, their physical mixture, freeze-dried blank SLNs powder and freeze-dried IBU-SLNs powder were determined by using a D8 ADVANCE powder X-ray diffractometer (Germany BRUKER) at room temperature. The Cu-Ka radiation was employed as the source of X-rays with an operating voltage of 40kV and electricity setting of 30mA. Samples were scanned over a range of 3°–60° 2θ angle at a scanning rate of 0.1/second and a step size of 0.010°.[35]

Fourier Transform Infrared (FTIR) Spectroscopy

FTIR spectra were obtained with the Fourier transform infrared spectrometer (Thermo Fisher, Nicolet iS50) over the region of 4000–400 cm^{-1}. All the samples were crushed in an agate mortar and separately mixed with KBr at a ratio of 1:20 (analyte: KBr, w/w). It is then compressed into a transparent disc for FTIR detection.[19]

Preparation of Thermosensitive in situ Gel (ISG)

In this study, as previously described by Choi et al, a thermosensitive in-situ gel based on weight/volume was prepared by the improved cold method, which contained a quantitative amount of the optimized IBU-SLNs (4mg/mL).[11] Briefly, 18% P407 (w/w) and 10% P188 (w/w) were gradually added to a cold optimized IBU-SLNs, stored at 4°C and mixed periodically until it was dissolved completely. Then, 0.2% HA (w/w) was added to the solution under stirring quantitatively to mix well and stored in the refrigerator at 4°C until a homogenous dispersion without clumps was obtained, and then, IBU-SLN-ISG was formed. In addition, the IBU in situ gel (IBU-ISG) was prepared in the same way as IBU-SLN-ISG to compare its properties with IBU-SLN-ISG in vitro and in vivo. The calculated amount of P407, P188 and HA was dispersed in cold ultrapurified water at 4°C, stored in a refrigerator, and mixed regularly until fully swollen. Then added the prescribed amount of IBU, to obtain a homogeneous IBU-ISG.[9] The compositions of gels are given in Table 3. Pediatric ibuprofen suppository was fused to prepare suppository for mice.

Table 3 The Gel Properties of the Formulation ($\overline{X}$±SD, n=3)

Formulation	P407/P188 (%, w/w)	Drug Form	Gelation Temperature (°C)	Gelation Time (s)	Gel Strength(s)	Bioadhensive Force (×10^2dyne/cm^2)
IBU-SLN-ISG1	18%/8%	SLNs	32.20±0.56	17.67±2.08	42.33±1.53	10.57±0.3
IBU-SLN-ISG2	18%/10%	SLNs	33.30±0.78	14.67±2.52	54.00±1.41	11.54±0.37
IBU-ISG1	18%/8%	PD	35.05±0.67	38.67±1.53	28.50±3.54	6.71±0.90
IBU-ISG2	18%/10%	PD	35.58±2.68	34.33±1.15	34.00±2.83	7.93±0.64

Note: 0.2% hyaluronic acid was added to each formulation.
Abbreviations: SLNs, solid lipid nanoparticles; PD, pure drug.

Characterization of Thermosensitive in situ Gel

Measurement of Gelation Temperature and Gelation Time

The gelation temperature and gelation time were measured by the stirring magnetic bar method.[25,57] Briefly, a transparent vial containing a magnetic bar and 10 mL of the thermosensitive gel was placed in a low-temperature intelligent Magnetic Stirrer (SNCL). A digital thermosensor connected to a thermistor was immersed in the ISG solution. In situ gel solution was heated at a rate of 1–2°C/min with the continuous stirring of 50 rpm. When the magnetic bar stopped moving due to gelation, the temperature displayed on the thermistor was determined as the gelation temperature. Briefly, a vial containing 10 mL of formulation and a magnetic bar was immersed in a thermostated bath at 37°C, under continuous stirring at 50 rpm. The time at which the magnetic bar stopped shaking, as a consequence of gelation, was recorded as the gelation time. The gelation temperature and gelation time results are the mean of three separate determinations.

Measurement of Gel Strength

The gel strength was evaluated using the method described by Chio et al.[10] The formulation (50 g) was p[illegible] in a 100-m[illegible] graduated cylinder and gelled in a thermostat at 34°C. The apparatus (weight: 35 g) for measuring gel stre[illegible]th was the[illegible]placed[illegible] the gelled solution. The gel strength was determined by the time (s) the apparatus took to sink 5 cm d[illegible]wn throu[illegible] the ge[illegible] cases where it took more than 300 s to drop the apparatus into the gel, various weights were placed on t[illegible] to[illegible] of the a[illegible]paratus, and the gel strength was described by the minimal weights that pushed the apparatus 5 cm dow[illegible] through the[illegible]l. Th[illegible] gel strength measuring device is shown in Figure 1.

Measurement of Bioadhesive Force

The bioadhesive force of the in situ gel formulation was determ[illegible]ed by usin[illegible] a modified mucoadhesion measurement device.[10] Porcine rectal mucosa was mounted on two glass vials, r[illegible]pectively. T[illegible]e vial was placed at 32–34°C for 10 min to maintain its overall temperature around 33°C, preven[illegible]ting hydrati[illegible]of th[illegible] in situ gel during the measurement. A vial was attached to one side of the balance and a 0.5 mL s[illegible]mple[illegible] the gel was placed between two mucous membranes

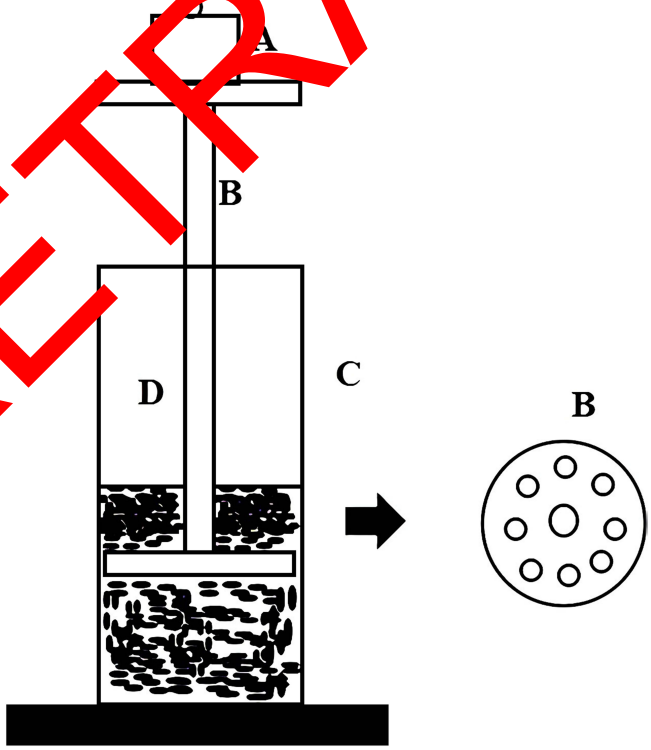

Figure 1 Gel strength measuring device; (**A**) weights; (**B**) device; (**C**) mess cylinder; (**D**) poloxamer gel.

attached to the bottom of the vial. Bioadhesive force, the detachment stress (dyne/cm^2), was determined from the minimal weights that detached the two vials. The gel bioadhesion measurement setup is shown in Figure 2.

Measurement of Rheological Properties

The rheological behavior of IBU-SLN-ISG and IBU-ISG was investigated at 37°C using a modern rheometer MCR101 (Anton Paar, Austria) with a plate diameter of 50 mm and a cone Angle of 4°. The sample (1.2 g) was allowed to stand on the plate for 60 s to eliminate the external force caused by placing the sample on the plate and to keep the sample in a homogeneous temperature. Next, the corresponding elastic and loss modulus of the in-situ gel was determined isothermally at 37°C by working at a shear rate of 0–100.$^{-1}$ [29] We research the changes of elastic modulus, loss modulus and angular frequency, strain through amplitude sweep and frequency sweep. Viscosity measurement is performed at 37°C, which represents physiological body temperature. The rheometer was used for viscosity measurement at a f[illegible]ear rate of 100 s^{-1}.

In vitro Drug Release

Release studies were performed to evaluate the in vitro drug release pattern using th[illegible] dialysis bag [illegible]eth[illegible].[36] The dialysis bags with a molecular weight cutoff of 12~14 kDa were soaked in a release m[illegible]ium fo[illegible]2 hours [illegible]efore use. 5 mL of each test formulation were individually placed in a dialysis bag. Both sides o[illegible] the d[illegible]is bag w[illegible]e tied up with a thread to prevent leakage. They were then immersed in 900 mL of phosphate [illegible]ffered solu[illegible]n (p[illegible] 6.8) maintained at 37°C ±0.5°C with stirring at 50 rpm in a dissolution tester (Vision classic 6, Hanso[illegible] America). At predetermined time points, 1 mL of the sample was withdrawn, and the volume was replaced with the sa[illegible] volume of fresh medium. The IBU concentration of the samples was determined by HPLC after [illegible]ltration through a membrane (Φ=0.45 μm). All experiments were performed in triplicate.

The release mechanism of mucoadhesive in situ gels with[illegible] without [illegible]pids by a model function was attempted by three mathematical models, namely zero, first-orde[illegible]netics, Hig[illegible]odel and Ritger-Peppas model that were often used to describe the drug release behavior from poly[illegible]eric s[illegible]ms. The mechanism of ibuprofen release from the solid lipid nanoparticle in situ gel is by fitting the release ra[illegible]ata to the following equation:[22]

$$\frac{M_t}{M_\infty} = kt^n \quad (1)$$

or the logarithmic form of t[illegible] equatio[illegible]

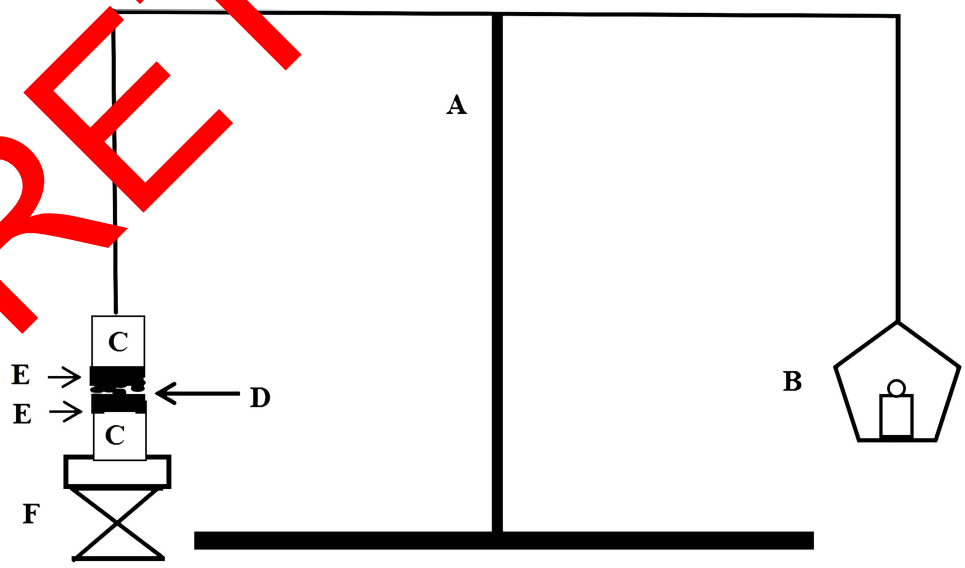

Figure 2 Bioadhesive force-measuring device, (**A**) modified balance; (**B**) weights; (**C**) glass vial; (**D**) poloxamer gel; (**E**) nasal mucosa; (**F**) height-adjustable pan.

$$\log \frac{M_t}{M_\infty} = \log k + n \log t \quad (2)$$

where M_t/M is the fraction of released drug at time t, k is a characteristic constant of the liquid suppositories, n is an indicator of the release mechanism. As the k value becomes higher, the drug is released faster. The n value of 1 corresponds to zero-order release kinetics, $0.5 < n < 1$ means a non-Fickian release model, and $n = 0.5$ indicates Fickian diffusion (Higuchi model).

Pharmacokinetic Study

Animal Studies

Eighteen male Sprague-Dawley rats weighing 240 ±10 g was used for this study. They were randomly divided into three groups (IBU-SLN-ISG, IBU-ISG, IBU-suppository), and fasted for 24 h prior to drug administration but allowed free access to water.

Each rat, anesthetized in an ether-saturated chamber, was secured on a surgical board in the supine position with a thread. A polyethylene tube was inserted into the right femoral artery of the rat. The animals were given ibuprofen supposity, and those in IBU-SLN-ISG group or IBU-ISG group (30 mg/kg IBU) were administered respectively, into the rectum 4 cm above the anus through a stomach sonde needle fitted with a glass syringe. IBU solid suppository was administered with a dose of 0.56 g/kg (equivalent to IBU 30 mg/kg) into the rectum 4 cm above the anus. The entrance of the anus was then blocked with a cyanoacrylate adhesive to prevent the suppositories from leaking out from the anus. Blood samples (0.2 mL) were collected into anticoagulant centrifuge tubes from the right femoral artery at various intervals (5, 15, 30, 45, 60, 90, 120, 240, 360 min). Plasma was separated by centrifugation at 13,000 rpm for 10 min using a centrifuge 5810R and stored in plastic tubes at −20°C until analysis.[37]

Blood Sample Analysis

A 50 µL aliquot of each plasma sample, 10 µL flufenamic acid solution (130 ng/mL) as an internal standard (IS) working solution, and 200 µL acetonitrile were pipetted into a 1.5 mL eppendorf tube. After vortexing for a few minutes, the tube centrifuged at 13,000 rpm for 10 min to precipitate the protein. The supernatant layer (200 µL) was transferred to a clean eppendorf tube and evaporated under a stream of nitrogen gas at 30°C. The residue was reconstituted in 100 µL of mobile phase. Each mixture was vortexed for 3 min and centrifuged at 13,000 rpm for 10 min. And then each supernatant was injected into the UPLC-MS system for analysis.[39]

UPLC-MS/MS Method

The Shimadzu UPLC system (Shimadzu, Kyoto, Japan) and AB SCIENX 4500 mass spectrometer (Shimadzu, Kyoto, Japan) were used to quantitatively analyze IBU in the biological samples. The analyses were conducted on AB SCIEX QTRAP 4500 triple quadrupole UPLC-MS/MS system (USA) operated in electrospray ionization (ESI) (−) mode. The optimized chromatographic separation of IBU was performed by using Ultimate XB-C18 column (50 mm × 2.1 mm, 1.8 µm particle size) at a column temperature of 30°C. The mobile phase was prepared by gradient elution with 0.2% formic acid dissolved in water (mobile phase A) and acetonitrile (mobile phase B). The flow rate was 0.3 mL/min. The elution program was 0.01 min (5%B), 0.5–2.0 min (80% B), 2.01–3.00 min (80–60% B), 3.01–3.5 minutes (60–40%B), 3.51–4.0 minutes (40–30% B), 4.01–4.5 minutes (30–5%B), 4.5–5.0 (5%B). The most abundant fragment ions in multiple reaction monitoring (MRM) were adopted, and m/z 205.0 → m/z 161.0 for IBU and m/z 280.1 → m/z 236.0 for IS at a collision energy of −10 V and −25 V were monitored. Declustering potential of IBU and IS was −107 V and −90 V, respectively. The total run time of the assay was 5.0 min. The retention time of IBU was 1.77 minutes, and the retention time of the IS was 1.82 minutes. The ion spray voltage was adjusted at 3.0 kV. The common parameters were as follows: nebulizer gas pressure was 45 psi; gas temperature was 550°C; curtain gas, 20 arbitrary units; GS1, 45 arbitrary units and GS2, 50 arbitrary units.

The linear concentration range of ibuprofen in rat plasma was 0.01–100 µg/mL with a lower limit of quantification (LLOQ) of 0.1µg/mL (R = 0.9958). The mean IBU plasma extraction recovery was (93.13 ± 9.84) %, while (94.48 ± 10.07) % of the internal standard was recovered. The intra-day precision was about 15% at the quantitation limit (100 ng/mL) and less than 10% at higher concentrations. And the inter-day precision of low, medium and high concentrations was 16.98%, 11.29%, and 11.36%, respectively.

Pharmacokinetic Analysis

The plasma IBU concentrations were evaluated using the equation from the standard curves that were run with each batch of samples. The plasma concentration–time data were analyzed with the Drug and Statistics 2.0 software package to determine the pharmacokinetic parameters. The maximum plasma concentration (C_{max}, μg/mL) and the time to reach the maximum concentration (T_{max}, h) were calculated using the rat plasma concentration–time curve. According to the linear trapezoidal rule, we add the areas from 0 to t h to get the area under the curve from 0 to t (AUC_{0-t}).

Histopathological Studies

Animal rectum segment from the IBU-SLN-ISG or IBU-ISG groups were collected immediately after 6 h of rectal administration. The rectum was separated, rinsed with saline solution, and immersed in 10% neutral carbonate-buffered formaldehyde, embedded in paraffin and cut into slices. The slices were stained with hematoxylin-eosin and examined under a light microscope.[39]

Rectal Retention Study

Male, Sprague-Dawley rats weighing 240 ± 10 g, were fasted for 24 h prior to the experiments but were allowed free access to water. The IBU-SLN-ISG formulation was mix with 0.1% methylene blue dye and administered at a dose of 1.5 g/kg into the rectum 4 cm above the anus, using a stomach sonde needle. After 30 min and 6 h after administration, observe the hair color around the anus to determine whether the gel has leaked from the anus, and the localization of IBU-SLN-ISG formulation in the rectum was identified by the presence of the blue dye.[35]

Statistical Analysis

All data were analyzed as mean values ± SD. Statistical analysis was performed using the SPSS 26.0 software, and comparisons among groups were performed using an independent sample *t* test. The P-value of 0.05 was considered statistically significant.

Results and Discussion

Experimental Data Analysis and Validation

Seventeen experimental runs were conducted to analyze the effects of three formulation variables on five response variables (Table 2). Based on the data obtained, the fitting models of polynomial equations involving the main effects and interaction factors for EE, DL, MPS, PDI and ZP were statistically analyzed by calculating the P-values with a 95% confidence level. The quadratic model was found to be significant for EE, DL and MPS. The values of R^2 showed a good

Table 4 Summary of Results of Regression Analysis for the Considered Responses R1-R5

Factors	EE (R1)		DL (R2)		MPS (R3)		PDI (R4)		ZP (R5)	
	Coefficient	*P*-value	Coefficient	*P*-value	Coefficient	*P*-value	Coefficient	*P*-value	Coefficient	*P*-value
Model		0.0011*	9.25	0.0039*	5.43	0.0181*	1.53	0.2932	1.27	0.3831
A	1.5	0.2599	2.74	0.1417	9.03	0.0198*	1.66	0.2386	0.23	0.6464
B	12.48	0.0096*	3.85	0.0907	0.15	0.714	4.27	0.0776	2.57	0.153
C	3.16	0.0002*	1.24	0.3029	12.77	0.009*	2.18	0.1834	0.26	0.6226
AB	6.19	0.0417*	9.78	0.0167*	0.82	0.394	0.071	0.7981	1.36	0.2821
AC	11.6	0.0113*	2.93	0.1309	0.74	0.4182	0.9	0.3743	0.7	0.4301
BC	10.06	0.0157*	0.039	0.8481	0.0055	0.9429	0.7	0.4313	0.3	0.6017
A^2	6.07	0.0433*	12.8	0.009*	0.88	0.3793	2.08	0.1928	3.28	0.1128
B^2	8.68	0.0215*	6.63	0.0367*	23.96	0.0018*	0.87	0.3811	2.33	0.1705
C^2	15.66	0.0055*	37.69	0.0005*	0.085	0.7797	1.19	0.3117	0.28	0.6115
Lack of Fit	1.23	0.4076	0.59	0.6509	1.22	0.4102	6.68	0.0489	20.98	0.0066
R^2	0.9465		0.9225		0.8748		0.6635		0.621	

Notes: *Significant value, with a 95% confidence interval. R^2 is the correlation coefficient.

correlation between the response and selected variables (Table 4). The values of the obtained responses varied from 72.72% to 90.28% for EE, from 7.04% to 14.94% for DL, from 89.3 to 273.67 nm for MPS, from 0.24 to 0.77 for PDI, from −24.37 to −15.0 mV for ZP. It was seen that the quadratic model was best fitted for both the responses studied. The quadratic model generated for both responses was as follows:

$$EE(\%) = 87.71 + 0.71A + 2.05B + 4.03C + 2.05AB + 2.8AC - 2.01BC - 1.97A^2 - 2.36B^2 - 3.17C^2$$

$$DL(\%) = 13.66 - 0.68A + 0.80B - 0.46C + 1.81AB + 0.99AC - 0.12BC - 2.02A^2 - 1.46B^2 - 3.46C^2$$

$$MPS(nm) = 219.08 + 36.97A - 4.7B - 43.97C - 15.8AB - 14.97AC + 1.29BC - 15.91A^2 - 83.02B^2 + 4.93C^2$$

$$PDI = 0.52 + 0.06A - 0.096B - 0.069C - 0.018AB - 0.063AC - 0.055BC - 0.092A^2 - 0.0[illegible]07C^2$$

$$ZP(mV) = -20.42 - 0.39A + 1.3B - 0.42C + 1.33AB + 0.96AC + 0. + 0.63BC + 2.02A[illegible] 1.7B^2 - 0.5[illegible]C^2$$

The effect of the amount of SA (A) in the dependent variables was shown in Tables 4. The factor positively influenced the EE (R1) and MPS (R3) of IBU-SLNs, since the P-values were <0.05 with a 95% confidence interval. It meant that this response increased as the amount of SA increased. And the amount of GMS (B) in the dependent variables only positively influenced the EE (R1). The effect of the amount of Tween 80(C) was statistically significant (P-value <0.05) for the EE (R1) and MPS (R3). It is also shown that the interaction between the two factors has a significant effect on EE ($P < 0.05$).

Based on the polynomial models, the results of three-dimensional response surface analysis were plotted (from Figures 3–5), representing the effect of significant independent factors on each observed response. The 3D response surface of (C) is significantly steeper in Figure 3, indicating that the influence of GMS and Tween-80 on EE is greater than that of A. It was also observed that as the lipid amount increased, the EE of SLNs also increased. This may be due to the increased internal phase, as more amounts of lipids were available for the dissolving of lipophilic drug IBU.[30] The increase in entrapment efficiency upon increasing Tween 80 concentration could be attributed to the added emulsification and stabilization effect of this lipid material in the presence of Tween 80.[31]

The DL depends on the solubility of the drug in the solid lipid. Lipid crystalline structure has been correlated with drug loading and release behavior. Some researchers reported that amorphous structure provides superior drug loading and retention than more crystalline structure.[32] The3D response graph (Figure 4) showed that with the increasing use of lipid and surfactant in formulations, DL (R2) increased first and decreased later, which indicated that it was important to find a balance between the amount of excipients and DL.

The 3D surface plots were generated to describe the interaction between the study factors and analyzed their influence on the MPS of SLN (Figure 5). It is shown that, when the amount of Tween 80 increases, the particle size of SLN decreases. Higher amounts of surfactant were able to reduce the size of SLNs. This effect is related to higher amount of surfactant which may promote formation and stabilization of smaller particles due to the decrease in interfacial tension between the lipid and the aqueous phase and, consequently, control the aggregation of lipid particles.

Numerical optimization based on the desirability function approach was utilized to predict the optimum formulation composition with maximized encapsulation efficiency, maximized drug loading and minimized size. The optimum SLN was formulated with 0.20 g of SA, 0.25 g of GMS, and 0.55 g of Tween 80. The EE%, DL% and MPS of optimized IBU-SLNs were (90.74 ± 1.40) %, (11.36 ± 1.20) % and (166.77 ± 2.26) nm, respectively, which are shown in Table 5. The observed values of the responses were found to be nearly close to their predicted values. Moreover, the calculated prediction error (%) values indicated good reliability of the model.

SEM Analysis

SEM has been widely used to acquire information on the size, shape, and surface morphology of nanoparticles. Figure 6 shows that IBU-SLNs were spherical or nearly spherical with a smooth surface (Figure 6). No major differences were detected between the blank SLNs and IBU-SLNs.

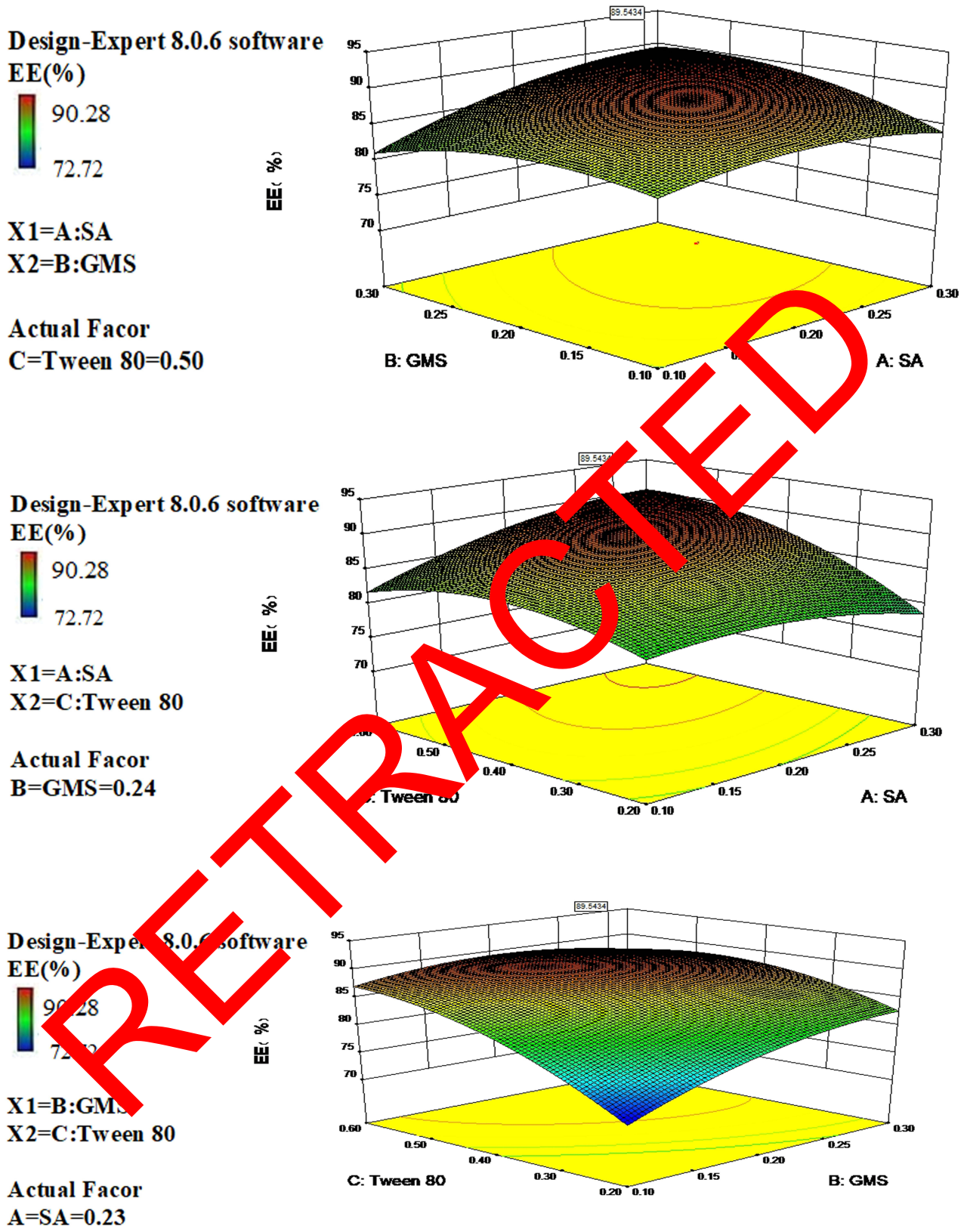

Figure 3 Three-dimensional surface and interaction plots showing the effects of the independent variables on entrapment efficiency of IBU-SLNs.

Figure 4 Three-dimensional surface and interaction plots showing the effects of the independent variables on drug loading of IBU-SLNs.

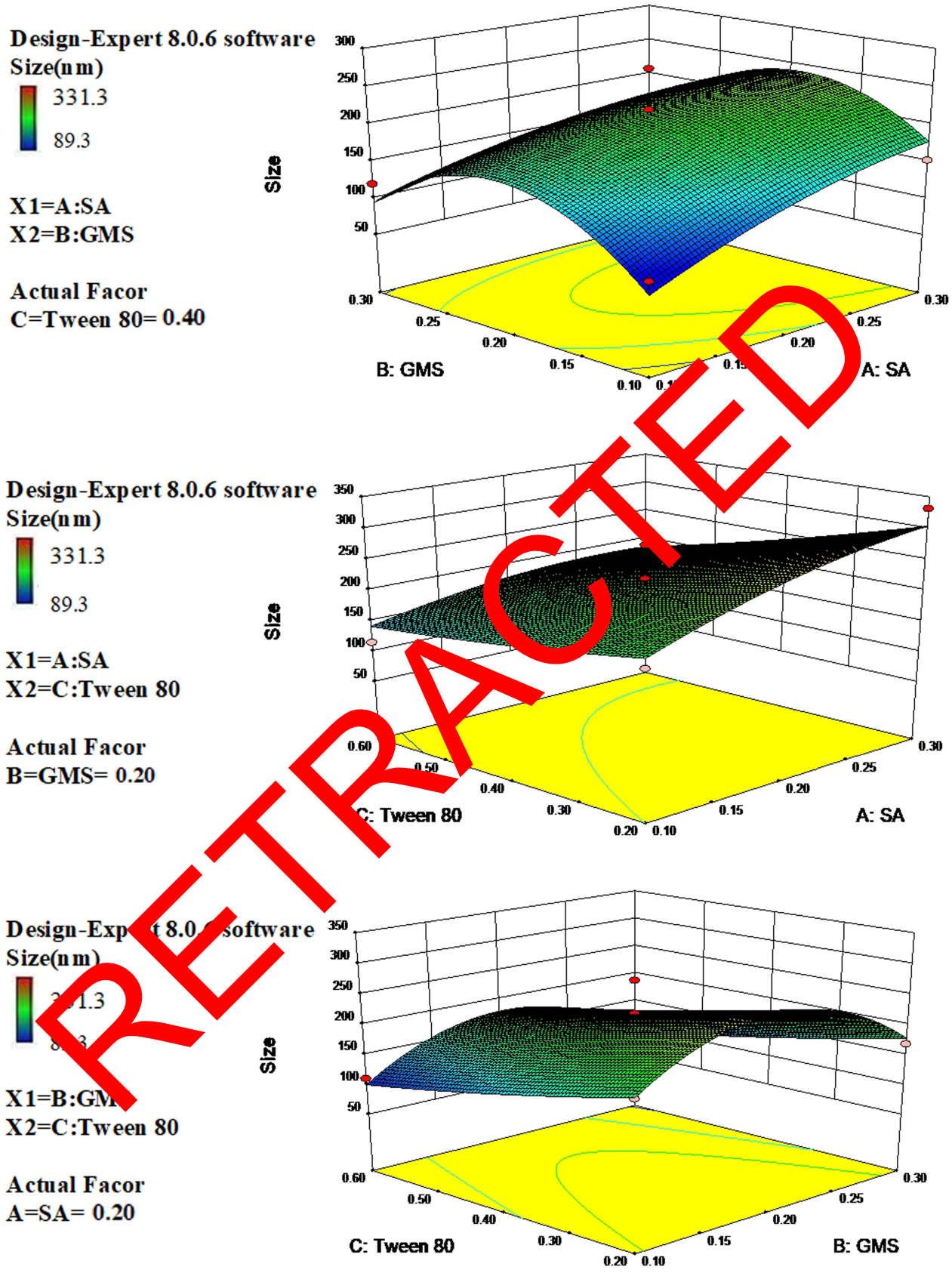

Figure 5 Three-dimensional surface and interaction plots showing the effects of the independent variables on mean particle size of IBU-SLNs.

Table 5 Predicted versus Observed Values of Optimized IBU-SLNs

Dependent Variables	Predicted	Observed	Prediction Error (%)
R1=entrapment efficiency(%)	89.54	90.74±1.40	1.32
R2=loading efficiency (%)	11.60	11.36±1.20	2.11
R3=mean particle size (nm)	165.21	166.77±2.26	0.94
R4=polymer dispersity index	0.26	0.27±0.08	3.70
R5=zeta potential (mV)	−20.73	−21.00±0.59	1.28

X-RAD Analysis

Since the change in crystallinity is an indicator of the formation of SLNs, X-ray powder diffraction patterns of pure IBU, SA, GMS, their physical mixtures and IBU-SLNs are shown in Figure 7. The characteristic peaks of IBU showed sharp peaks at diffraction angles (2θ) of 6.0°, 12.0°, 16.0°, 17.0°, 19.0°, 21.0°, 24.0°, 25.0° and 27.0°, indicating that the drug exists as a crystalline substance. The diffraction pattern of the bulk lipid matrix showed remarkable difference from the SLNs, where the lipids had sharp peaks. The diffraction pattern exhibited by the physical mixture can be characterized as a superposition of crystalline IBU and lipids. In contrast, the diffraction pattern of IBU-SLNs is amorphous and only characterized by large diffraction peaks, while the characteristic peaks of IBU and lipids do not exist.[40] The disappearance of IBU peak observed in the IBU-SLNs indicated that there was no IBU peak in the crystalline state in the SLNs.[41] This may be attributed to the incorporation of IBU into the lipid matrix and successful encapsulation of the drug inside the lipids.[42] The X-ray results confirmed that the drug was in the molecular dispersion or amorphous state in SLNs, which facilitated the diffusion of drug molecules through the polymer matrix, thus improving the dissolution rate of poorly soluble drugs and continuously releasing them from the SLNs.[43]

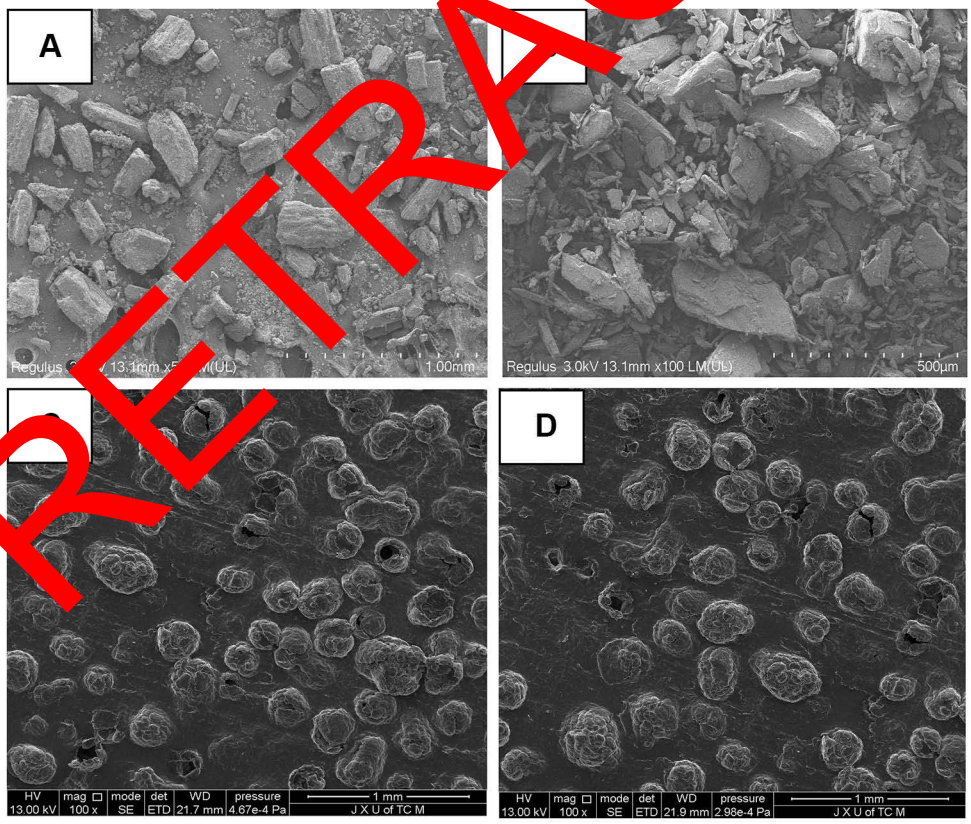

Figure 6 Scanning electron microscope micrograph of (**A**) pure ibuprofen, (**B**) a physical mixture (between the lipids and ibuprofen), (**C**) Freeze-dried IBU-loaded SLNs, (**D**) Freeze-dried blank SLNs.

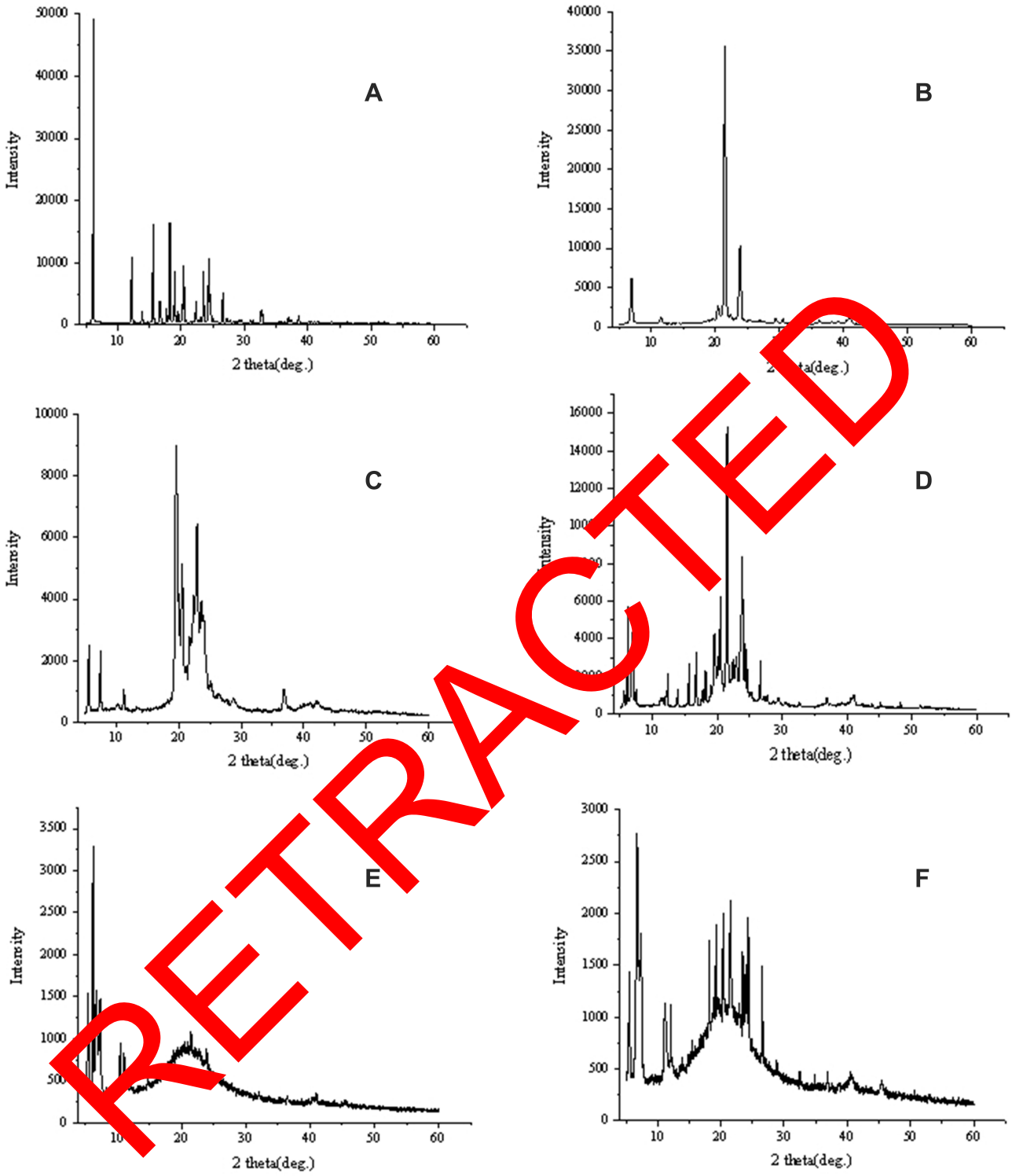

Figure 7 X-ray diffraction patterns of (**A**) ibuprofen, (**B**) stearic acid (SA), (**C**) glyceryl monostearate (GMS), (**D**) a physical mixture of lipid and ibuprofen, (**E**) freeze-dried IBU-SLN and (**F**) freeze-dried blank SLN.

FTIR Analysis

Molecular interactions between components in SLNs were characterized by FTIR spectra. Fourier transform infrared spectroscopy (FTIR) was also used to determine the functional groups present on the surface of the nanoparticle. The

FTIR spectrums of pure IBU, pure SA, pure GMS, physical mixture (between the lipid and IBU), IBU-SLNs and blank SLNs are presented in Figure 8. The characteristic peaks of IBU were at 1651 cm^{-1} (carboxylic acid group - COOH) and 1226 cm^{-1} (C = C group of aromatic rings). GMS produced characteristic absorption peaks at wavelengths of 2916.57 cm^{-1} (C-H, stretching), 1729.67 cm^{-1} (carbonyl group C=O, stretching) and 1178 cm^{-1} (C-O, stretching). The FTIR spectrum of SA showed the characteristic peaks of broad C-H stretching at 2915.71 cm^{-1}, C=O stretching at 1699.64 cm^{-1}. The spectrum of the physical mixture shows retention of the characteristic peak of ibuprofen with a slight shift indicating no chemical interaction between IBU and excipients. And the FTIR spectra of IBU-SLNs showed characteristic carbonyl peaks (carbonyl group C=O) for lipid and IBU were shifted and overlapped. There was a small peak/shoulder, which was characteristic to the drug, and a significant shift occurred in their position compared to the native spectrum of IBU. The intensity of this peak was low, indicating that IBU was captured in the lipid.[21,44] The FTIR spectra confirmed successful encapsulation of the drug inside the nanoparticle as only peaks responsible for the lipid could be identified. This corroborated well with XRD spectra, which showed a completely amorphous state of the IBU-loaded nanoparticles as compared to the crystalline nature of the pure drug. The presence of characteristic peaks of pure lipid and IBU as well as formulation revealed that the specific functional groups of lipid material on the nanoparticle surface had almost the same chemical characteristics as the pure lipid.[41] This FTIR spectrum suggested that molecular interactions that could change the chemical structure of the IBU did not occur. Therefore, there was no chemical interaction between the functional groups of the drug and the added excipients, which was consistent with the literature.[44]

Gel Properties Analysis

IBU-SLN-ISG was evaluated in terms of gelation temperature and gel time. For liquid suppository, gelation temperature ranged 30–36°C. Choi et al reported that the use of P407 or P188 alone did not provide a liquid suppository with an appropriate gelling temperature. It has been reported that when P407 and 188 were used together, as the concentration of P407 increases, the mixture required a smaller amount of P188 to gel at the ideal gelation temperature.[25] Our previous study showed that the gelation temperature of in situ gels increased gradually with the increase in the proportion of P407, and gradually increased with the increase in the proportion of P188. Our study indicated that when the ratio of P407 to P188 was 18/10, the gelation temperature of 35°C was suitable.[14,44] Therefore, a combination of 18% P407 and 10% P188 was used in our study, in which 0.2% HPMC was added. This means that the formula is liquid at room temperature and turns into a gel instantly at physiological temperature. In this study, the gelation time of the IBU-SLN-ISG and IBU-ISG was about 15 s and 34 s, indicating its speedy gelation.[55]

The two most important indexes of gel degree are strength and bioadhesive force. Appropriate strength and bioadhesion can ensure the retention of gel in the administration position for a long time, increase the rectal absorption time, and improve the rectal absorption efficiency.[56] Bioadhesion refers to the binding force of a liquid suppository to rectal mucosa at 36.5°C.[57] It has previously been reported that poloxamer with hydrophilic oxide groups can bind to the oligosaccharides on the rectal mucosa and produce moderate bioadhesion. The stronger the biological adhesion, the more it can prevent the gel suppository to the colon end, that is, the first pass effect.[58] However, if the bioadhesive force is too large, the gel will damage the rectal mucosa. Therefore, liquid suppositories must have a suitable bioadhesive force. Our results show that IBU-SLN-ISG has a suitable gel temperature (30–33°C), gel strength (54.00 ± 1.41s) and bioadhesion (11.54 ± 0.37 dyne/cm^2). IBU-SLN-ISG was easily administered to the anus and remains in the administration site without leakage. In addition, this suppository with rectal mucosa adhesion cannot reach the colon end, resulting in that the drug delivered may not have a first-pass effect.

Rheological Properties Analysis

Rheological status is an important physical parameter in the development of a potential new drug delivery system for topical use. The rheological behavior of IBU-SLN-ISG was evaluated. In order to measure linear viscoelasticity, the linear viscoelastic region needs to be determined. We take ibuprofen in situ gel to determine this area by measuring G′ and G″ as a function of strain amplitude.[45] Figure 9A shows the different in situ gel energy storage (G′) and loss (G″) modulus and shear strain amplitude γ relationship. Based on the measurement results, the maximum deformation of the three-dimensional network structure inside the gel could be obtained, and the amplitude sweep were carried out (strain is

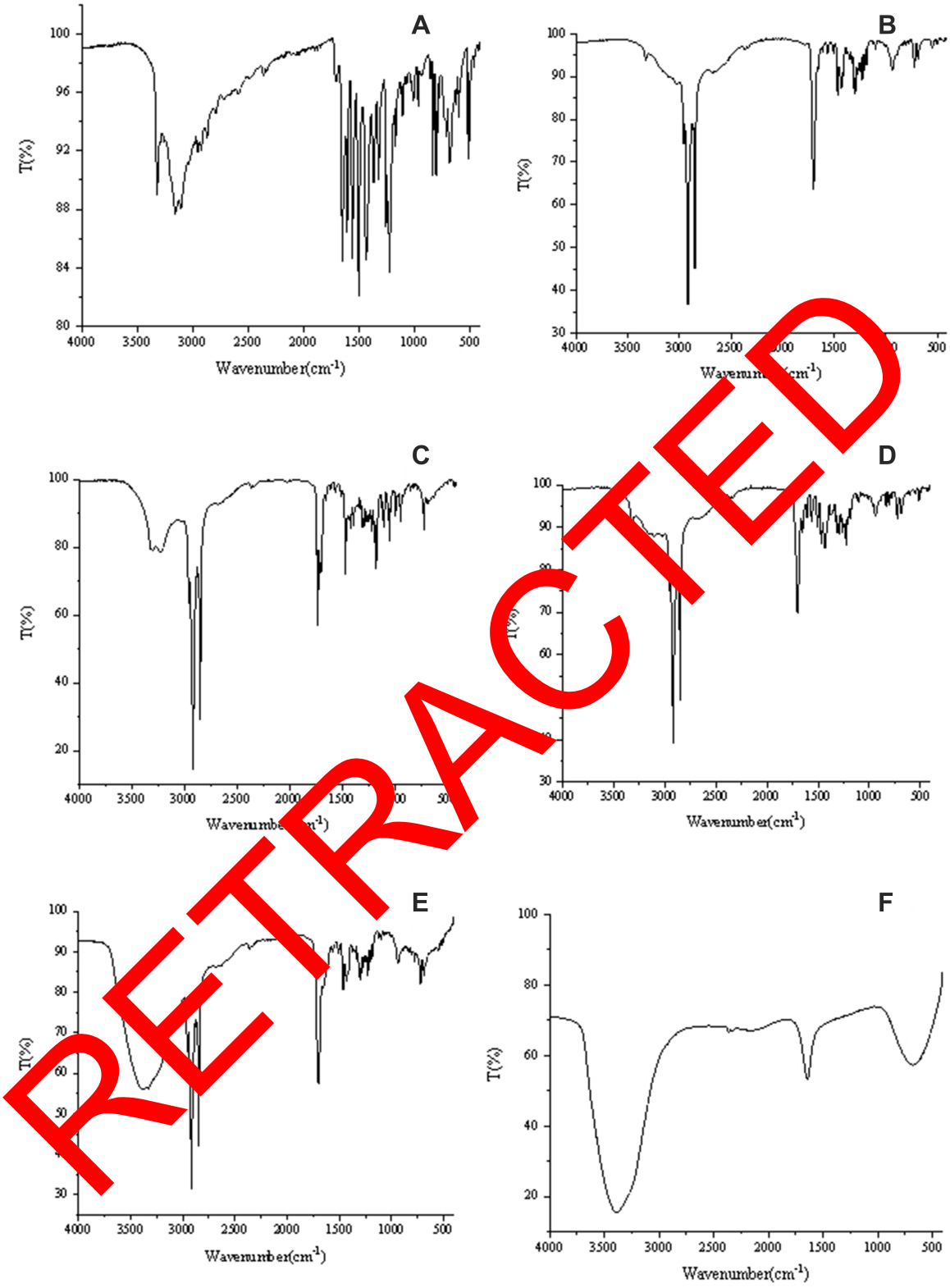

Figure 8 Fourier transform infrared spectroscopy spectra of (**A**) pure ibuprofen, (**B**) stearic acid, (**C**) glyceryl monostearate, (**D**) a physical mixture of lipid and ibuprofen, (**E**) ibuprofen-loaded solid lipid nanoparticles and (**F**) blank solid lipid nanoparticles.

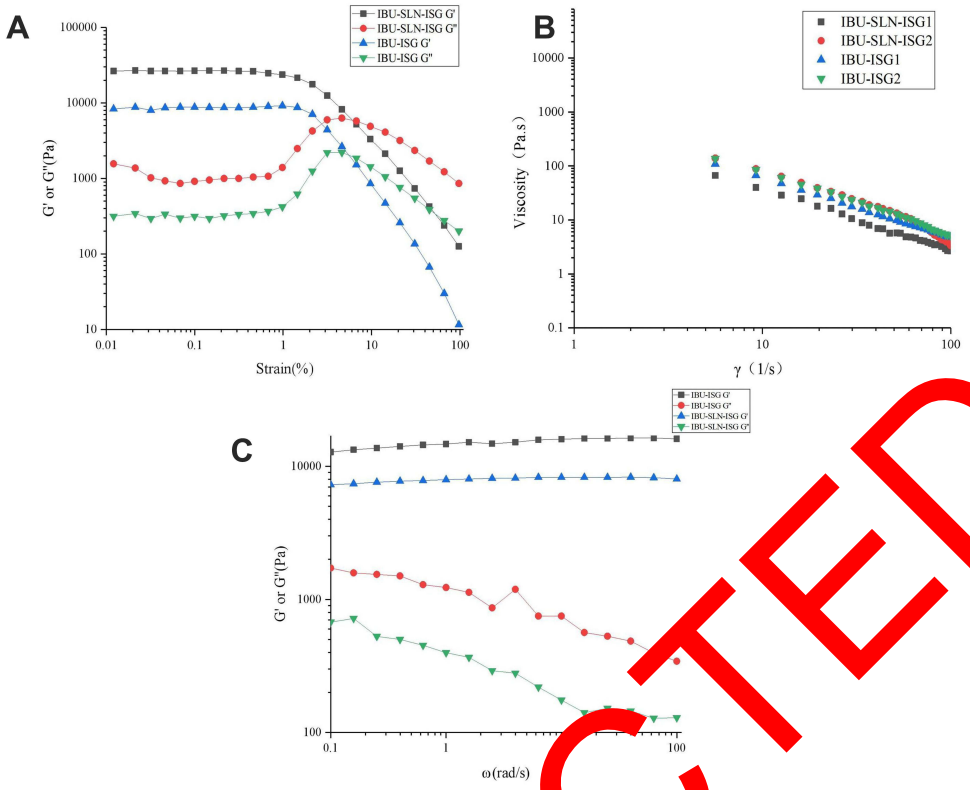

Figure 9 Rheological properties of IBU-SLN-ISG and IBU-ISG. (**A**) Strain-sweep measurements of IBU-SLN-ISG and IBU-ISG; (**B**) Shear rate viscosity measurements at 37 °C; (**C**) Oscillating measurement of the IBU-SLN-ISG and IBU-ISG. The oscillating frequency was 10 rad/s and the temperature of 37°C. Elastic and viscosity moduli at 37 °C as a function angular frequency.

0.01% to 100%, frequency is 10 rad/s). It has been observed that G′ and G″ are constant between 0.1% and 1% strain amplitude. Therefore, a strain amplitude of 1% was selected for all dynamic measurements. It can be seen from the figure that the strain (γ)<10%, G′>G″, elasticity was the main component, that is, the sample exhibited a gel structure, when γ>10%, G′ started to decrease, and when G′=G″, it condensed the glue structure was completely destroyed, G'<G", viscosity is the main body, showing fluid properties.

Gel strength is the viscosity of a liquid suppository at physiological temperature.[51] Shear rate viscosity was measured at 37°C. The gel viscosity curve and the measured viscosity values are shown in Figure 9B and Table 6, respectively. The viscosity of gels decreased with the increase in shear rate (γ), showing pseudoplasticity.[47] This rheological property had less irritation to the rectum and was more acceptable to patients; in addition, it also made the gel solution easy to stir and fill, thus reducing the difficulty and cost of industrial production.

Figure 9C shows the measurement of elastic modulus (G′) and loss modulus (G″) of IBU-SLN-ISG and IBU-ISG. These measurements were performed at 37°C.[48] Figure 9C indicates that both IBU-SLN-ISG and IBU-ISG were

Table 6 Shear Rate-Dependent Viscosity (Pa·s) for the Formulation at 37°C

Sample	Shear Rate (s^{-1})				
	0.1	5	10	50	100
IBU-SLN-ISG1	3260	66.6	39.8	5.72	2.64
IBU-SLN-ISG2	7200	138	87.8	13.2	3.37
IBU-ISG1	4110	109	84.9	9.87	4.81
IBU-ISG2	6730	136	84.9	13	5.1

viscoelastic fluid. In the entire frequency scan range, G′ was always greater than G”; that is, its elastic component was greater than its viscous component, showing that obviously elasticity was the main characteristic. And G′ did not change with ω, while G″ decreased with ω, and there was no significant frequency dependence, indicating that the gel always had a stable three-dimensional network structure.[49] Oscillatory measurements by varying the frequency showed that the elastic modulus of the IBU-ISG formulations was higher than IBU-SLN-ISG. It is shown that IBU-ISG has stronger rigidity and greater hardness than IBU-SLN-ISG.

In vitro Drug Release Study

The in vitro release profiles of the different formulations are shown in Figure 10. The cumulative percentage releases of IBU from IBU-SLN, IBU-SLN-ISG, and IBU-ISG were 93.86 ± 2.71%, 85.62 ± 2.14% and 72.82 ± 5.87%, respectively, within the time course of the study. In the first 2 hours, the release of the drug from the SLN-ISG formulation was approximate 22%, and it increased over time after 2 hours. This may be due to the slow diffusion of the drug from the lipid matrix.[49] In the drug release mode of the IBU-SLN formulation, a biphasic pattern was characterized by an initial burst release and subsequent delayed release. The initial rapid release stage may be due to the lipid soft shell and its ability to promote high solubility of lipophilic drugs or the presence of free drug IBU in the external phase and on the surface of SLN, resulting in a burst drug release phenomenon.[50] Meanwhile, the relative fast release at the initial stage might also be due to the nanoparticles having large specific surface area and some IBU molecules absorbed on the surface of nanoparticles. Moreover, osmotic pressure difference, namely, the drug concentration in the dialysis bag was higher than the drug concentration in the mediator, leading to drug fast release into the release medium as well.[51] IBU-SLNs increased the solubility of IBU, resulting in a higher and faster drug release rate and dissolution rate. The release of IBU in IBU-SLN-ISG was slower than IBU-SLNs, which may be due to the slow-release effect of the polymer matrix. The dissolution rate of IBU in IBU-SLN-ISG was the slowest among IBU-SLNs and IBU-SLN-ISG, which may be due to the poor water solubility of IBU.

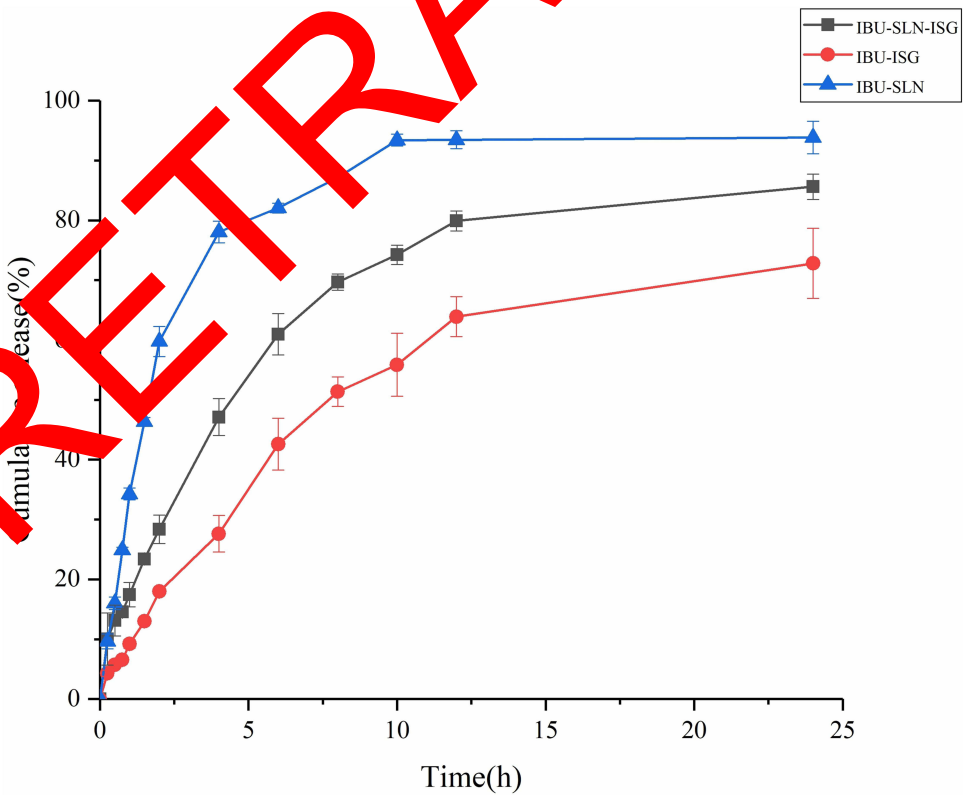

Figure 10 In vitro drug release profiles of IBU from different formulation in phosphate buffer. (Data has been represented as the mean ± SD; n = 3).

The release data were analyzed with zero-order kinetic, first-order kinetic, Higuchi kinetic and Ritger-Peppas kinetic models.[51,52] The R^2 value for each model is presented in Table 7. It can be seen from the fitting results that R^2 is 0.9936, indicating that the Fickian diffusion (Higuchi model) can better fit the in vitro drug release of IBU-SLN-ISG.[10] The Higuchi model describes the mechanism of controlled drug release, where the concentration of the drug in the matrix is lower than its solubility, and the drug occurs by diffusing through channels in the membrane.[53] The result may be attributed to the reduced particle size and spherical shape of IBU-SLNs, resulting in an increase in the solubility of IBU in the lipid matrix, so that the Higuchi model better describes the release behavior of IBU-SLN-ISG.[54] Table 7 shows that the n values of IBU-ISG were close to 0.5, suggesting that IBU might be released from the ISG by Fickian diffusion through extramicellar aqueous channels of the gel matrix, which means the outer layer of poloxamer cross-linking system.[11]

Results of Pharmacokinetic Study

The plasma concentration–time curves are plotted in Figure 11, and the main pharmacokinetic parameters are summarized in Table 8. The plasma concentration of IBU in the IBU-SLN-ISG was significantly higher than that of IBU-ISG and IBU solid suppository at each observing time.

According to the C_{max} and AUC values, IBU-SLN-ISG could achieve faster absorption and higher serum levels of IBU. The results showed that the mean residence time (MRT) and elimination half-life $t_{1/2}$ of rectal IBU-SLN-ISG and IBU- ISG were 8.63 h and 4.31 h, 6.83 h and 4.9 h, respectively. The $AUC_{(0-\infty)}$ value of IBU-SLN-ISG (136.28 ± 27.33 μg·h/mL) was significantly higher than that of IBU-ISG (80.77 ± 56.87 μg·h/mL) ($P < 0.05$) and IBU-suppository (41.39 ± 17.08μg·h/mL) ($P < 0.01$). Compared with IBU-ISG group (39.51 ± 1.27 μg·h/mL), the $AUC_{(0\rightarrow t)}$ (59.34 ± 26.57 μg·h/mL) of the IBU-SLN-ISG group increased about 70.76%. The IBU-SLN-ISG gave a significantly higher $AUC_{(0\rightarrow t)}$ value compared to the IBU-suppository (59.34 ± 26.57 vs 18.94 ± 3.33 μg·h/mL) (Table 8), leading to the improvement of 3.13-fold bioavailability, indicating that IBU-SLN-ISG could enhance the bioavailability of IBU.

Pharmacokinetic studies have shown that, compared with IBU solid suppositories, IBU-SLN-ISG successfully increased the bioavailability of ibuprofen by about 3.13 times and $t_{1/2}$ to about 6.83 hours. Compared with IBU suppository, after rectal administration of IBU-SLN-ISG, the $t_{1/2}$ and MRT of IBU were prolonged, and the $AUC_{(0-\infty)}$ was significantly increased, indicating that IBU-SLN-ISG could improve the drug delivery at the administration site. The retention time was longer, and it had the effect of slow and controlled release, which could reduce the frequency of IBU administration. In contrast, compared with ibuprofen in situ gel, IBU-SLN-ISG significantly increased the area under the curve (AUC) and mean residence time (MRT) of IBU drug. Plasma C_{max} reached (18.04 ± 1.29μg/mL) after IBU-SLN-ISG administrated (Table 8). The MRT of IBU in IBU-SLN-ISG (8.63 h) was significantly longer than that of IBU suppository (2.69 h) ($P < 0.01$). The elimination t½ time for IBU was also significantly ($p < 0.01$) longer after the IBU-SLN-ISG compared with the suppository. These results indicated that the former absorbs IBU faster than the latter. The reason for this difference may be the presence of lipid matrix. The drug in IBU-SLN-ISG slowly dissolves and then disperses in the rectum. On the contrary, the IBU-ISG is directly dispersed into the rectum, gels and adheres to the rectal mucosa. These results indicated that in-situ gels based on solid lipid nanoparticles would be useful to deliver IBU because it could increase the water solubility of IBU and prolong absorption. The experimental

Table 7 The Mathematical Model Fitting of Release Kinetics of IBU from Different Formulations

Model	IBU-SLN-ISG	IBU-ISG	IBU-SLN
Zero-order kinetic	$M_t = 3.83t + 19.70$ R^2=0.7567	$M_t = 3.39t + 10.24$ R^2=0.8376	$M_t = 3.86t + 34.51$ R^2=0.5721
First-order kinetic	$\ln M_t = 0.21t + 85.64$ R^2=0.9398	$\ln M_t = 0.13t + 77.68$ R^2=0.9618	$\ln M_t = 1.25t + 92.41$ R^2=0.9950
Higuchi kinetic	$\frac{M_t}{M_\infty} = 20.86\sqrt{t} + 0.99$ R^2=0.9936	$\frac{M_t}{M_\infty} = 17.78\sqrt{t} - 4.99$ R^2=0.9957	$\frac{M_t}{M_\infty} = 22.72\sqrt{t} + 12.46$ R^2=0.8293
Rigiter-Peppas kinetic	$\frac{M_t}{M_\infty} = 23.83t^{0.45}$ R^2=0.9462	$\frac{M_t}{M_\infty} = 13.93t^{0.56}$ R^2=0.9546	$\frac{M_t}{M_\infty} = 39.48t^{0.33}$ R^2=0.8816

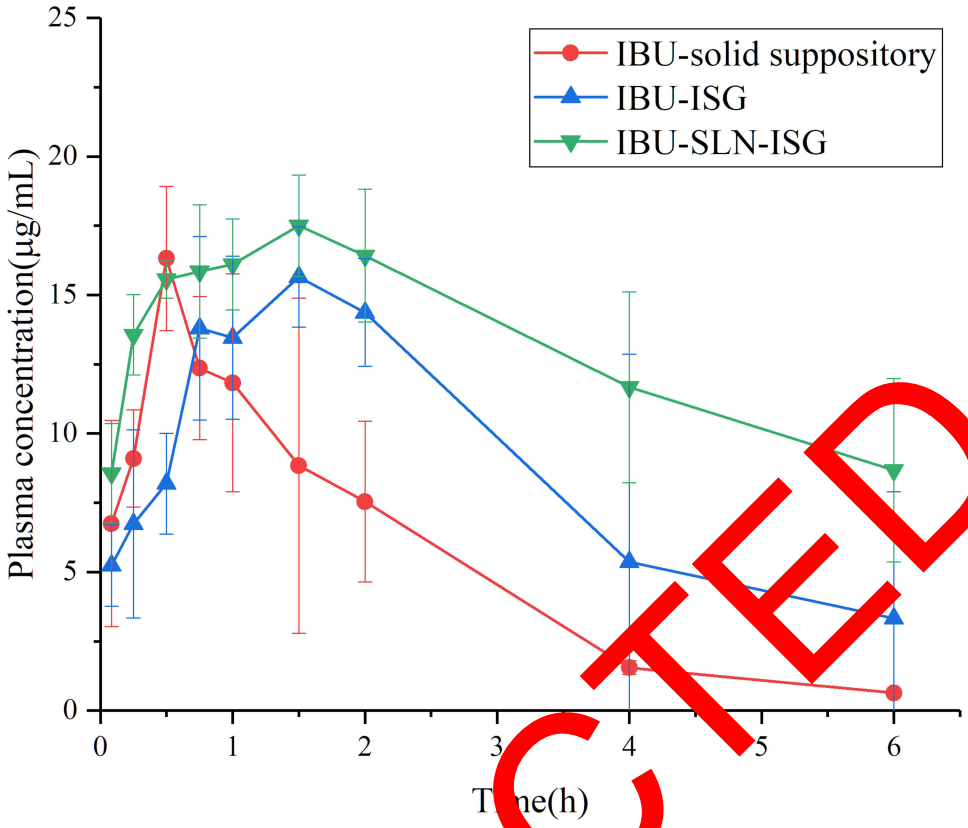

Figure 11 Mean plasma ibuprofen concentration after rectal administration of IBU formulations ($\bar{X}$±SD, n=6).

results showed that the preparation of IBU-SLN-ISG for rectal administration could increase the residence time of the drug at the drug site, increase the absorption of the drug, and significantly improve the bioavailability of IBU.

Histopathological Analysis

The safety test was performed to observe any irritation or damage to rectal tissues in rats after rectal administration of IBU-SLN-ISG. The results are shown in Figure 12. Rectal tissue morphological test showed that both IBU-ISG and IBU-SLN-ISG caused no irritation or damage to rectal tissues.

Result of Rectal Retention Study

The localization of IBU in the rectum was observed after mixing 0.1% of blue dye to IBU-SLN-ISG formulation.[57] 30 min after rectal administration, the blue color of IBU-SLN-ISG clearly showed in the rectum, and the color faded in the

Table 8 Pharmacokinetic Parameters of IBU in Serum After Rectal Administration ($\bar{X}$±SD, n=6)

Parameter	IBU-Suppository	IBU-ISG	IBU-SLN-ISG
C_{max}(μg/mL)	15.41±3.23	16.16±1.61	18.04±1.29
T_{max}(h)	0.60±0.14	1.25±0.35	1.50±0.00**$^{\#}$
t½(h)	1.68±0.50#	4.90±0.91**	6.83±1.92**
$AUC_{(0\rightarrow t)}$ (μg·h/mL)	18.94±8.33	39.31±1.27*	59.34±26.57*
$AUC_{(0\rightarrow\infty)}$ (μg·h/mL)	41.39±17.08	80.77±56.87*	136.28±27.33**#
$MRT_{(0\rightarrow\infty)}$(h)	2.69±0.78	4.31±4.13	8.63±4.09*#

Notes: *P<0.05, **P<0.01, vs IBU-suppository; $^{\#}$P<0.05, $^{\#\#}$P<0.01 vs IBU-ISG; $AUC_{(0\rightarrow\infty)}$, area under the plasma concentration time curve calculated by the trapezoidal rule from time 0 to infinity; SD, standard deviation; $t_{1/2}$, elimination half-life; C_{max} peak plasma concentration; T_{max}, time to reach peak plasma concentration; F_1 represent absolute bioavailability.

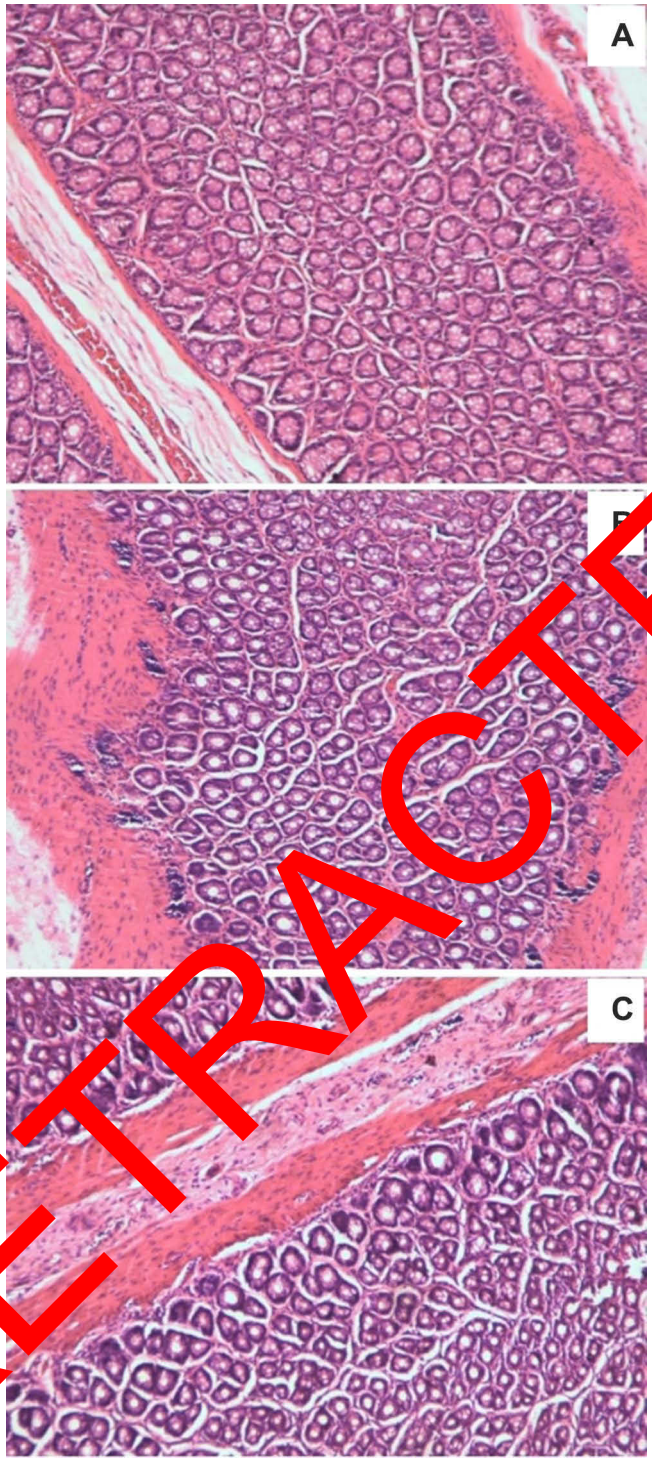

Figure 12 The morphology of rectal tissues after rectal administration of IBU-SLN-ISG and IBU-ISG: (**A**) control group, (**B**) 6 h after rectal administration of IBU-SLN-ISG, and (**C**) 6 h after rectal administration of IBU-ISG.

same position after 6 h (Figure 13). However, the position of IBU-SLN-ISG within the rectum did not change significantly over time, indicating that this formulation could be retained in the rectum for more than 6 hours. It indicated that the bioadhesive force of the IBU-SLN-ISG is strong enough to hold the gelled suppository in the rectum of rats for at least 6 h.

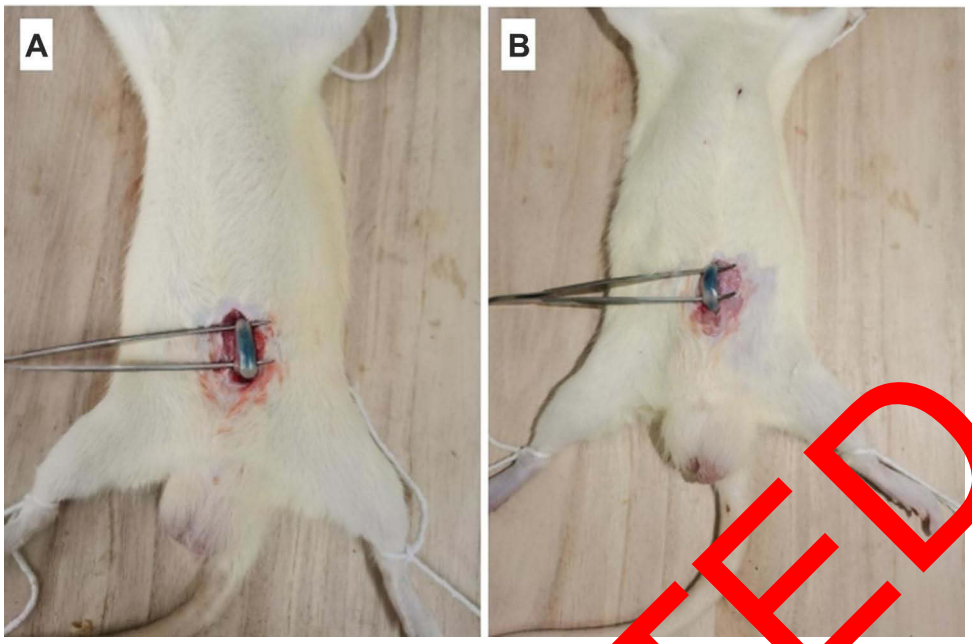

Figure 13 In vivo localization of IBU-SLN-ISG in the rectum at (**A**) 30 min and (**B**) 6 h after rectal administration. The IBU-SLN-ISG composed of IBU-SLN/P407/P188 with 0.1% methylene blue dye was administered into the rectum of rat. The localization of the formulation in the rectum was identified by a blue color.

Conclusion

Ibuprofen loaded SLNs were successfully developed, characterized and optimized employing Box-Behnken design for rectal delivery. The effect of formulation variables ie, the amount of SA, GMS and Tween 80 on EE, DL, MPS, PDI and ZP of SLNs was studied. The optimized SLNs were found to have desirable physicochemical properties. The SLNs were incorporated into thermosensitive gel which showed pseudoplastic flow behavior and fairly good texture for rectal application. The in vitro results of IBU-SLNs and IBU-SLN-ISG showed a biphasic release pattern with initial burst release followed by sustained release. More importantly, IBU-SLN-ISG produced much better absorption of IBU and improved bioavailability in rats. In addition, IBU-SLN-ISG caused no irritation or damage to rectal tissues, and could be retained in the rectum for a long time. These results suggested the potential application of IBU-SLN-ISG as a more convenient and effective rectal dosage form for non-steroidal anti-inflammatory use.

Disclosure

The authors report no conflicts of interest in this work.

References

1. Tarloff JB. Analgesics and nonsteroidal anti-inflammatory drugs. *Comprehensive Toxicol*. 2010;7:387–403. doi:10.1016/B978-0-08-046884-6.00821-6
2. Rainsford KD. Ibuprofen: pharmacology, efficacy and safety. *Inflammo -Pharmacol*. 2009;17(6):275–342. doi:10.1007/s10787-009-0016-x
3. Ozgüney I, Kardhiqi A, Yıldız G, Ertan G. In vitro–in vivo evaluation of in situ gelling and thermosensitive ketoprofen liquid suppositories. *Eur J Drug Metab Pharmacokinet*. 2014;39(4):283–291. doi:10.1007/s13318-013-0157-6
4. Bushra R, Aslam N. An overview of clinical pharmacology of ibuprofen. *Oman Medical Journa*. 2010;25(3):155–1661. doi:10.5001/omj.2010.49
5. Park YJ, Yong CS, Kim HM, et al. Effect of sodium chloride on the release, absorption and safety of diclofenac sodium delivered by poloxamer gel. *Int J Pharm*. 2003;263(1–2):105–111. doi:10.1016/S0378-5173(03)00362-4
6. El-Leithy ES, Shaker DS, Ghorab MK, Abdel-Rashid RS. Evaluation of mucoadhesive hydrogels loaded with diclofenac sodium–chitosan microspheres for rectal administration. *AAPS PharmSciTech*. 2010;11(4):1695–1702. doi:10.1208/s12249-010-9544-3
7. Yahagi R, Onishi H, Machida Y. Preparation and evaluation of double-phased mucoadhesive suppositories of lidocaine utilizing Carbopol and white beeswax. *J Control Release*. 1999;61(1–2):1–8. doi:10.1016/s0168-3659(99)00111-x
8. He C, Kim SW, Lee DS. In situ gelling stimuli-sensitive block copolymer hydrogels for drug delivery. *J Control Release*. 2008;127(3):189–207. doi:10.1016/j.jconrel.2008.01.005

9. Li L, Guo D, Guo J, et al. Thermosensitive in-situ forming gels for ophthalmic delivery of tea polyphenols. *J Drug Deliv Sci Technol*. 2018;46:243–250. doi:10.1016/j.jddst.2018.05.019
10. Kim CK, Lee SW, Choi HG, et al. Trials of in situ-gelling and mucoadhesive Acetaminophen liquid suppository in human subjects. *Int J Pharm*. 1998;174(1–2):201–207. doi:10.1016/S0378-5173(98)00258-0
11. Choi HG, Oh YK, Kim CK. In situ gelling and mucoadhesive liquid suppository containing Acetaminophen: enhanced bioavailability. *Int J Pharm*. 1998;165(1):23–32. doi:10.1016/S0378-5173(97)00385-2
12. El-Samaligy MS, Yahia SA, Basalious EB. Formulation and evaluation of diclofenac sodium buccoadhesive discs. *Int J Pharm*. 2004;286(1–2):27–39. doi:10.1016/j.ijpharm.2004.07.033
13. Patel A, Bell M, O'Connor C, Inchley A, Wibawa J, Lane ME. Delivery of ibuprofen to the skin. *Int J Pharm*. 2013;457(1):9–13. doi:10.1016/j.ijpharm.2013.09.019
14. Ryu JM, Chung SJ, Lee MH, Kim CK, Shim CK. Increased bioavailability of propranolol in rats by retaining thermally gelling liquid suppositories in the rectum. *J Controlled Release*. 1999;59(2):163–172. doi:10.1016/s0168-3659(98)00189-8
15. Koffi AA, Agnely F, Besnard M, KablanBrou J, Grossiord JL, Ponchel G. In vitro and in vivo characteristics of a thermogelling and bioadhesive delivery system intended for rectal administration of quinine in children. *Eur J Pharm Biopharm*. 2008;69(1):167–175. doi:10.1016/j.ejpb.2007.09.017
16. Barichello JM, Morishita M, Takayama K, Chiba Y, Tokiwa S, Nagai T. Enhanced rectal absorption of insulin-loaded pluronic f-127 gels containing unsaturated fatty acids. *Int J Pharm*. 1999;183(2):125–132. doi:10.1016/s0378-5173(99)00090-3
17. Yun M, Choi H, Jung J, Kim C. Development of a thermo-reversible insulin liquid suppository with bioavailability enhancement. *Int J Pharm*. 1999;189(2):137–145. doi:10.1016/s0378-5173(99)00227-6
18. Uchida T, Toida Y, Sakakibara S, et al. Preparation and characterization of insulin-loaded acrylic hydrogel containing absorption enhancers. *Chem Pharm Bull (Tokyo)*. 2001;49(10):1261–1266. doi:10.1248/cpb.49.1261
19. El-Kamel A, El-Khatib M. Thermally reversible in situ gelling carbamazepine liquid suppository. *Drug Deliv*. 2006;13(2):143–148. doi:10.1080/10717540500316003
20. Ivanova NA, Trapani A, Franco CD, et al. In vitro and ex vivo studies on diltiazem hydrochloride-loaded microsponges in rectal gels for chronic anal fissures treatment. *Int J Pharm*. 2019;557:53–65. doi:10.1016/j.ijpharm.2018.12.039
21. Barakat NS. In vitro and in vivo characteristics of a thermogelling rectal delivery system of etodolac. *AAPS PharmTech*. 2009;10(3):724–731. doi:10.1208/s12249-009-9261-y
22. Yuan Y, Cui Y, Zhang L, et al. Thermosensitive and mucoadhesive in situ gel based on poloxamer as new carrier for rectal administration of nimesulide. *Int J Pharm*. 2012;430(1–2):114–119. doi:10.1016/j.ijpharm.2012.03.054
23. Kim JK, Kim MS, Park JS, et al. Thermo-reversible flurbiprofen liquid suppository with hp-β-cd as a solubility enhancer: improvement of rectal bioavailability. *J Incl Phenom Macrocycl Chem*. 2009;64(3–4):265–272. doi:10.1007/s10847-009-9560-7
24. Reanmongkol W, Kaewnopparat N, Ratanajamit C. Development of tramadol hydrochloride rectal gel preparations and evaluation of analgesic activity in experimental animals. *J Drug Deliv Sci Technol*. 2011;21(6):503–507. doi:10.1016/S1773-2247(11)50081-4
25. Choi HG, Jung JH, Ryu JM, et al. Development of in situ-gelling and mucoadhesive Acetaminophen liquid suppository. *Int J Pharm*. 1998;165(1):33–44. doi:10.1016/S0378-5173(97)00386-4
26. Mehnert W, Mäder K. Solid lipid nanoparticles: production, characterization and applications. *Adv Drug Deliv Rev*. 2001;47(2–3):165–196. doi:10.1016/s0169-409x(01)00105-3
27. Batool S, Zahid F, Ud-Din F. Macrophage targeting with the novel cationic polymer-based miltefosine-loaded transfersomal gel for the treatment of cutaneous leishmaniasis: in vitro and in vivo analyses. *Drug Dev Ind Pharm*. 2021;47(3):440–453. doi:10.1080/03639045.2021.1890768
28. Dumortier G, Grossiord JL, Zuber M. Rheological study of a thermoreversible morphine gel. *Drug Dev Ind Pharm*. 2008;17(9):1255–1265. doi:10.3109/03639049109043858
29. Pham CV, Van C, Thi HP, et al. Development of ibuprofen loaded solid lipid nanoparticle-based hydrogels for enhanced in vitro dermal permeation and in vivo topical anti-inflammatory activity. *J Drug Deliv Sci Technol*. 2020;57:101758. doi:10.1016/j.jddst.2020.101758
30. Baig MS, Ahad A, Aslam M, et al. Application of box–behnken design for preparation of levofloxacin-loaded stearic acid solid lipid nanoparticles for ocular delivery: optimization, in vitro release, ocular tolerance, and antibacterial activity. *Int J Biol Macromol*. 2016;85:258–270. doi:10.1016/j.ijbiomac.2015.12.077
31. Kishore N, Dhanalekshmi UM, Raju MD, Bhavani S, Reddy PN. Design and in vitro evaluation of solid-lipid nanoparticle drug delivery for aceclofenac. *J Dispers Sci Technol*. 2012;33(1):96–102. doi:10.1080/01932691.2010.534293
32. Alam S, Aslam M, Khan A, et al. Nanostructured lipid carriers of pioglitazone for transdermal application: from experimental design to bioactivity detail. *Drug Deliv*. 2014;23(2):60[illegible]. doi:10.3109/10717544.2014.923958
33. Dumont C, Bourgeois S, Fessi H, Bugas PY, Jannin V. In-vitro evaluation of solid lipid nanoparticles: ability to encapsulate, release and ensure effective protection of peptides in the gastrointestinal tract. *Int J Pharm*. 2019;565:409–418. doi:10.1016/j.ijpharm.2019.05.037
34. Wadetwar RN, Agrawal AR, Kanojiya PS. In situ gel containingBimatoprost solid lipid nanoparticles for ocular delivery: in-vitro and ex-vivo evaluation. *J Drug Deliv Sci Technol*. 2020;56:101575. doi:10.1016/j.jddst.2020.101575
35. Das S, Ng WK, Kanaujia P, et al. Formulation design, preparation and physicochemical characterizations of solid lipid nanoparticles containing a hydrophobic drug: effects of process variables. *Colloids Surf B Biointerf*. 2011;88(1):483–489. doi:10.1016/j.colsurfb.2011.07.036
36. Kumar R, Singh A, Sharma K, Dhasmana D, Garg N, Siril PF. Preparation, characterization and in vitro cytotoxicity of fenofibrate and nabumetone loaded solid lipid nanoparticles. *Mater Sci Eng C*. 2020;106(C):110184. doi:10.1016/j.msec.2019.110184
37. Liu Y, Wang X, Liu Y, Di X. Thermosensitive in situ gel based on solid dispersion for rectal delivery of ibuprofen. *AAPS PharmSciTech*. 2018;19(1):338–347. doi:10.1208/s12249-017-0839-5
38. Din FU, Mustapha O, Kim DW, et al. Novel dual-reverse thermosensitive solid lipid nanoparticle-loaded hydrogel for rectal administration of flurbiprofen with improved bioavailability and reduced initial burst effect. *Eur J Pharm Biopharm*. 2015;94:64–72. doi:10.1016/j.ejpb.2015.04.019
39. Moawad FA, Ali AA, Salem HF. Nanotransfersomes-loaded thermosensitive in situ gel as a rectal delivery system of tizanidine hcl: preparation, in vitro and in vivo performance. *Drug Deliv*. 2017;24(1):252–260. doi:10.1080/10717544.2016.1245369
40. Xing R, Mustapha O, Ali T, et al. Development, characterization, and evaluation of SLN-loaded thermoresponsive hydrogel system of topotecan as biological macromolecule for colorectal delivery. *Biomed Res Int*. 2021;24(2021):1–14. doi:10.1155/2021/9968602

41. Akbari Z, Amanlou M, Karimi-Sabet J, et al. Production of ibuprofen-loaded solid lipid nanoparticles using rapid expansion of supercritical solution. *J Nano Res*. 2015;31:15–29. doi:10.4028/www.scientific.net/JNanoR.31.15
42. Potta SG, Minemi S, Nukala RK, et al. Preparation and characterization of ibuprofen solid lipid nanoparticles with enhanced solubility. *J Microencapsul*. 2011;28(1):74. doi:10.3109/02652048.2010.529948
43. Kumar R, Singh A, Garg N, Siril PF. Solid lipid nanoparticles for the controlled delivery of poorly water soluble non-steroidal anti-inflammatory drugs. *Ultrason Sonochem*. 2018;40(Pt A):686–696. doi:10.1016/j.ultsonch.2017.08.018
44. Omwoyo WN, Moloto MJ. Encapsulation of ibuprofen into solid lipid nanoparticles for controlled and sustained release using emulsification solvent evaporation technique. *Asian J Pharm Clin Res*. 2019;74–81. doi:10.22159/ajpcr.2019.v12i18.33652
45. Ricci EJ, Bentley M, Farah M, et al. Rheological characterization of poloxamer 407 lidocaine hydrochloride gels. *Eur J Pharm Sci*. 2002;17 (3):161–167. doi:10.1016/S0928-0987(02)00166-5
46. Chen L, Han X, Xu X, et al. Optimization and evaluation of the thermosensitive in situ and adhesive gel for rectal delivery of budesonide. *AAPS PharmSciTech*. 2020;21(3):97. doi:10.1208/s12249-020-1631-5
47. Rençber S, Karavana SY, Şenyiğit ZA, Eraç B, Limoncu MH, Baloğlu E. Mucoadhesive in situ gel formulation for vaginal delivery of clotrimazole: formulation, preparation, and in vitro/in vivo evaluation. *Pharm Dev Technol*. 2016;22(4):1–11. doi:10.3109/10837450.2016.1163385
48. Sun Y, Li L, Xie H, et al. Primary studies on construction and evaluation of ion-sensitive in situ gel loaded with pa[illegible]d solid lipid nanoparticles for intranasal drug delivery. *Int J Nanomedicine*. 2020;15:3137–3160. doi:10.2147/IJN.S247935
49. Baloglu E, Karavana SY, Senyigit ZA, Guneri T. Rheological and mechanical properties of poloxamer mixture[illegible]s a mucoadhe[illegible]e gel base. *Pharm Dev Technol*. 2011;16(6):627–636. doi:10.3109/10837450.2010.508074
50. Dudhipala N, Veerabrahma K. Candesartan cilexetil loaded solid lipid nanoparticles for oral delive[illegible] charac[illegible]ization, ph[illegible]macokinetic and pharmacodynamic evaluation. *Drug Deliv*. 2016;23(2):395–404. doi:10.3109/10717544.2014.914986
51. Wang F, Chen L, Jiang S, et al. Optimization of methazolamide-loaded solid lipid nanoparticles fo[illegible]ophthalmi[illegible]delivery [illegible] box-behnken design. *J Liposome Res*. 2014;24(3):171–181. doi:10.3109/08982104.2014.891231
52. Oshiro A, da Silva DC, de Mello JC, et al. Pluronics f-127/l-81 binary hydrogels as drug-de[illegible]ery sy[illegible] influence[illegible] physicochemical aspects on release kinetics and cytotoxicity. *Langmuir*. 2014;30(45):13689–13698. doi:10.1021/la5[illegible]021c
53. Costa P, Sousa Lobo JM. Modeling and comparison of dissolution profiles. *Eur J Pharm[illegible]*. [illegible]01;13(2):123–[illegible]:10.1016/s0928-0987(01)00095-1
54. Abioye AO, Issah S, Kola-Mustapha AT. Ex vivo skin permeation and retention st[illegible]ies on c[illegible]san–ibuprofen–gellan ternary nanogel prepared by in situ ionic gelation technique—a tool for controlled transdermal delivery of ibuprofen. *Int[illegible]Pharm*. 2015;490(1–2):112–130. doi:10.1016/j.ijpharm.2015.05.030
55. Din FU, Choi JY, Kim DW, et al. Irinotecan-encapsulated double-reverse[illegible]ermosensitive nanocarrier system for rectal administration. *Drug Deliv*. 2017;24(1):502. doi:10.1080/10717544.2016.1272651
56. Seo YG, Kim DW, Yeo WH, et al. Docetaxel-loaded thermosensitive an[illegible]ioadhesivenan[illegible]micelles as a rectal drug delivery system for enhanced chemotherapeutic effect. *Pharm Res*. 2013;30(7):1860–1870. doi:10.1007/[illegible]0095-013-1[illegible]9-0
57. Din FU, Kim DW, Choi JY, et al. Irinotecan-loaded double-[illegible]ible thermog[illegible]mproved antitumor efficacy without initial burst effect and toxicity for intramuscular administration. *Acta Biomaterialia*. [illegible]017;[illegible]30–248. doi:10.1016/j.actbio.2017.03.007
58. Yong CS, Oh YK, Jung SH, et al. Preparation of ibuprofen-load[illegible]liqui[illegible]supp[illegible]ory using eutectic mixture system with menthol. *Eur J Pharm Sci*. 2004;23(4–5):347–353. doi:10.1016/j.ejps.2004.08.008